

1 Confidence as a noisy decision reliability estimate

2 **Zoe M. Boundy-Singer^{1,2}, Corey M. Ziembra^{1,2}, Robbe L. T. Goris^{1*}**

3 ¹ Center for Perceptual Systems, The University of Texas at Austin, Austin, TX USA. ² These authors contributed equally *
4 email: robbe.goris@utexas.edu

5 **Decisions vary in difficulty. Humans know this and typically report more confidence in easy than in difficult**
6 **decisions. However, confidence reports do not perfectly track decision accuracy, but also reflect response**
7 **biases and difficulty misjudgments. To isolate the quality of confidence reports, we developed a model of**
8 **the decision-making process underlying choice-confidence data. In this model, confidence reflects a sub-**
9 **ject's estimate of the reliability of their decision. The quality of this estimate is limited by the subject's un-**
10 **certainty about the uncertainty of the variable that informs their decision ("meta-uncertainty"). This model**
11 **provides an accurate account of choice-confidence data across a broad range of perceptual and cognitive**
12 **tasks, revealing that meta-uncertainty varies across subjects, is stable over time, generalizes across some**
13 **domains, and can be manipulated experimentally. The model offers a parsimonious explanation for the**
14 **computational processes that underlie and constrain the sense of confidence.**

15 Humans are aware of the fallibility of perception and cognition. When we experience a high degree of confidence in a perceptual
16 or cognitive decision, that decision is more likely to be correct than when we feel less confident¹. This "metacognitive" ability
17 helps us to learn from mistakes², to plan future actions³, and to optimize group decision-making⁴. There is a long-standing
18 interest in the mental operations underlying our sense of confidence⁵⁻⁷, and the rapidly expanding field of metacognition seeks
19 to understand how metacognitive ability varies across domains⁸, individuals⁹, clinical states¹⁰, and development¹¹.

20 Quantifying a subject's ability to introspect about the correctness of a decision is a challenging problem¹²⁻¹⁴. There exists
21 no generally agreed-upon method¹⁵. Even in the simplest decision-making tasks, several distinct factors influence a subject's
22 confidence reports. Consider a subject jointly reporting a binary decision about a sensory stimulus (belongs to "Category A"
23 vs "Category B") and their confidence in this decision. Confidence reports will reflect the subject's ability to discriminate
24 between both stimulus categories – the higher this ability, the higher the reported confidence¹⁶. They will also reflect the
25 subject's response bias (e.g., a large willingness to declare "high confidence" or "Category A")¹⁷⁻¹⁹. Yet, neither of these
26 factors characterizes the subject's metacognitive ability¹³.

27 Here, we introduce a method to quantify metacognitive ability on the basis of choice-confidence data. We propose that confi-
28 dence reflects a subject's estimate of the reliability of their decision²⁰, expressed in units of signal-to-noise ratio. This estimate
29 results from a computation involving the uncertainty of the decision variable that informed the subject's choice²¹. It follows that
30 metacognitive ability is determined by the subject's knowledge about this uncertainty, or lack thereof (i.e., uncertainty about
31 uncertainty, hereafter termed "meta-uncertainty"). The more certain a subject is about the uncertainty of the decision variable,
32 the lower their meta-uncertainty, and the better they are able to assess the reliability of a decision. We leverage modern com-
33 putational techniques to formalize this hypothesis in a two-stage process model that is rooted in traditional signal detection
34 theory²² and that can be fit to choice-confidence data (the "CASANDRE" or "Confidence AS A Noisy Decision Reliability
35 Estimate" model). The model predicts a systematic dependency of confidence on choice consistency²⁰ and naturally separates
36 metacognitive ability from discrimination ability and response bias.

37 We found that this model provides an excellent account of choice-confidence data reported in a large set of previously pub-
38 lished studies²³⁻²⁸. Our analysis suggests that meta-uncertainty provides a better metric for metacognitive ability than the
39 non-process-model based alternatives that currently prevail in the literature^{13,15}. Specifically, meta-uncertainty has higher test-
40 retest reliability, is less affected by discrimination ability and response bias, and has comparable cross-domain generalizability.
41 Meta-uncertainty is higher in tasks that involve more levels of stimulus uncertainty, implying that it can be manipulated exper-
42 imentally. Together, these results illuminate the mental operations that give rise to our sense of confidence, and they provide
43 evidence that metacognitive ability is fundamentally limited by subjects' uncertainty about the reliability of their decisions.

44 Results

45 In simple decision-making tasks, human confidence reports lawfully reflect choice consistency²⁰. Consider two example sub-
46 jects who performed a two-alternative forced choice (2-AFC) categorization task in which they judged on every trial whether a
47 visual stimulus belonged to category A or B, and additionally reported their confidence in this decision using a four-point rating
48 scale. Categories were characterized by distributions of stimulus orientation that were predominantly smaller (A) or larger (B)

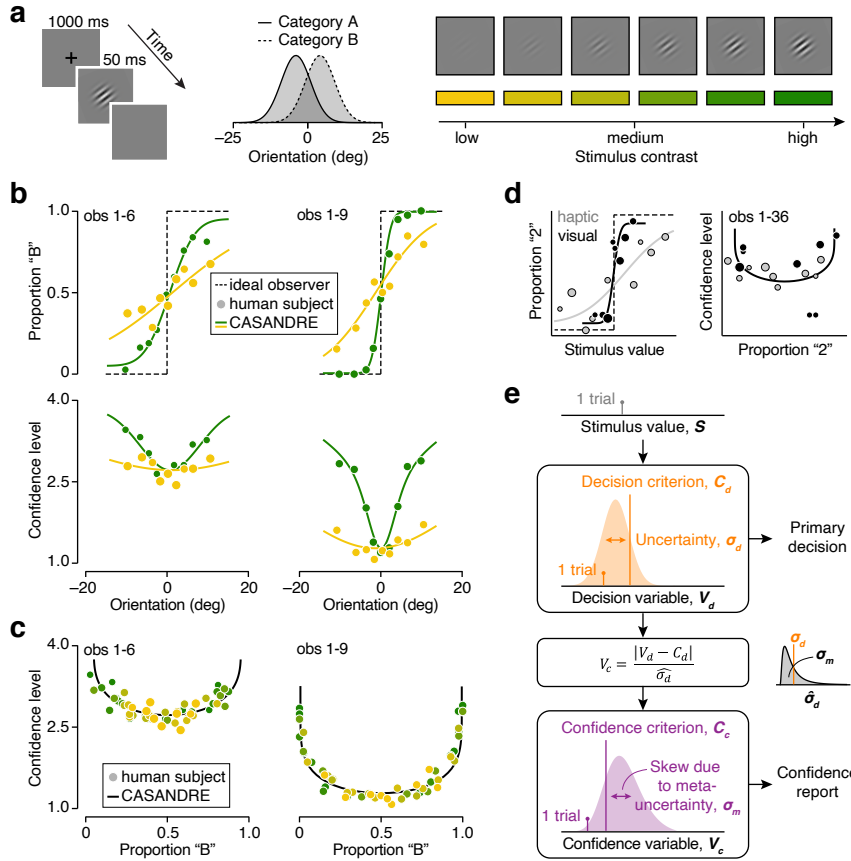


Figure 1 CASANDRE, a two-stage process model of decision confidence, accounts for the relation between confidence reports and choice consistency. **(a)** Experimental design employed by ref. ²⁵. **(b)** Top: Proportion of “Category B” choices is plotted against stimulus orientation, split out by stimulus contrast (green vs yellow), for two example subjects (left, obs 1-6: Observer 6 in experiment 1 from ref. ²⁵; right, obs 1-9: Observer 9 in experiment 1 from ref. ²⁵). Bottom: Same for mean confidence level. Symbols summarize observed choice behavior, the dotted line illustrates the theoretical optimum, and the full lines show the fit of the CASANDRE model. Symbol size is proportional to the number of trials. The model was fit to all data simultaneously using a maximum likelihood estimation method. Only two out of six contrasts are shown here. Fits to all conditions are shown in Supplementary Fig. 1. **(c)** Observed and predicted confidence-consistency relationship for two example subjects. **(d)** Observed and predicted choice-confidence data for an example subject performing a visuo-haptic two-interval forced choice (2-IFC) categorization task (observer 36 in experiment 1 from Arbuzova and Filevich in the Confidence Database ²³). **(e)** Schematic of the hierarchical decision-making process underlying choice-confidence data in the CASANDRE model.

than zero degrees. Stimuli varied in orientation and contrast (Fig. 1a). Because the category distributions overlap, errors are inevitable. The most accurate strategy is to choose category A for all stimuli whose orientation is smaller than zero degrees, and category B for all stimuli whose orientation exceeds zero degrees (Fig. 1b, top, dotted line). As can be seen from the aggregated choice behavior, the more the stimulus orientation deviates from zero, the more closely human subjects approximate this ideal (Fig. 1b, top, symbols). As can also be seen, this relationship is modulated by stimulus contrast – the lower the stimulus contrast, the weaker the association between orientation and choice (Fig. 1b, top, green vs yellow symbols). The distinct effects of orientation and contrast on choice consistency are evident in the subjects’ confidence reports. Confidence is minimal for conditions associated with a choice proportion near 0.5 (i.e., the most difficult conditions), and monotonically increases as choice proportions deviate more from 0.5 (Fig. 1b, bottom). We found that the association between choice consistency and confidence is so strong, that plotting average confidence level against the aggregated choice behavior reveals a single relationship across all stimulus conditions (Fig. 1c). This is true of both example subjects, although their confidence-consistency relationships differ in shape, offset, and range. We speculate that a lawful confidence-consistency relationship is not a coincidental feature of this experiment, but a widespread phenomenon in confidence studies (Fig. 1d).

A monotonically increasing relation between confidence reports and choice consistency implies that subjects can assess the reliability of their decisions. However, whether their ability to do so is excellent or poor cannot be deduced from empirical

64 measurements alone. One possibility is that subjects accurately assess decision reliability on every single trial, indicating excellent
65 metacognitive ability. Alternatively, there might be a high degree of cross-trial variability in confidence reports, implying less
66 accurate decision reliability assessment and thus limited metacognitive ability. Of course, given the variability of the primary
67 choice behavior, some variability in confidence reports is expected, even for flawless introspection. How much exactly?
68 And what might be the origin of excess variance? Answering these questions requires a quantitative model that provides an
69 analogy for the mental operations that underlie a subject's primary decisions and confidence reports. In the following section,
70 we develop such a process model.

71 **A two-stage process model of decision-making**

72 Assume that a subject solves a binary decision-making task by comparing a noisy, one-dimensional decision variable, V_d , to
73 a fixed criterion, C_d (Fig. 1e, top). For some tasks, it is convenient to think of this decision variable as representing a direct
74 estimate of a stimulus feature (e.g., orientation for the task shown in Fig. 1a). For other tasks, it is more appropriate to think
75 of it as representing the accumulated evidence that favors one response alternative over the other (e.g., "Have I heard this song
76 before?"). The process model specified by these assumptions has proven very useful in the study of perception and cognition.
77 It readily explains why repeated presentations of the same stimulus often elicit variable choices. In doing so, it clarifies how
78 choices reflect a subject's underlying ability to solve the task as well as their primary response bias²².

79 We expand this framework with an analogous second processing stage that informs the subject's confidence report. Assume
80 that the subject is presented with a set of stimuli that elicit the same level of cross-trial variability in the decision variable.
81 The smaller the overlap of the stimulus-specific decision variable distribution with the decision criterion, the "stronger" the
82 associated stimulus is, and the more consistent choices will be. On any given trial, the distance between the decision variable and
83 the decision criterion provides an instantaneously available proxy for stimulus strength, and hence for choice reliability^{14,29-33}.
84 However, in many tasks, the decision variable's dispersion, σ_d , will vary across conditions, resulting in different amounts of
85 stimulus "uncertainty" (the larger σ_d , the greater this uncertainty). To be a useful proxy for choice reliability, the stimulus
86 strength estimate must therefore be normalized by this factor²⁰. This operation yields a unitless, positive-valued variable, V_c ,
87 which represents the subject's confidence in the decision:

$$V_c = \frac{|V_d - C_d|}{\hat{\sigma}_d} \quad (1)$$

88 where V_d is the decision variable, C_d the decision criterion, and $\hat{\sigma}_d$ the subject's estimate of σ_d . We assume that the subject
89 is unsure about the exact level of stimulus uncertainty. Repeated trials will thus not only elicit different values of the decision
90 variable, but will also elicit different estimates of stimulus uncertainty. Specifically, we assume that $\hat{\sigma}_d$ is on average correct
91 (i.e., its mean value equals σ_d), but varies from trial-to-trial with standard deviation σ_m , resulting in "meta-uncertainty" (the
92 larger σ_m , the greater this meta-uncertainty). As we shall see, variability in the decision variable is the critical model component
93 that limits stimulus discriminability, while variability in the uncertainty estimate similarly limits metacognitive ability. Finally,
94 comparing the confidence variable with a fixed criterion, C_c , yields a confidence report (Fig. 1e, bottom).

95 To fit this model to data, the form of the noise distributions must be specified. A common choice for the first-stage noise is the
96 normal distribution. This choice is principled, as the normal distribution is the maximum entropy distribution for real-valued
97 signals with a specified mean and variance³⁴. It is also convenient, as it results in fairly simple data-analysis recipes²². The
98 second-stage noise describes variability of a positive-valued signal (σ_d cannot be smaller than zero by definition). A suitable
99 maximum entropy distribution for such a variable is the log-normal distribution^{28,34}. Under these assumptions, the confidence
100 variable is a probability distribution constructed as the distribution of the ratio of a normally and log-normally distributed
101 variable. There exists no closed form description of this ratio distribution, ruling out simple data-analysis recipes. However,
102 we can leverage modern computational tools to quickly compute the confidence variable's probability density function by
103 describing it as a mixture of Gaussian distributions (see Methods). This mathematical street-fighting maneuver³⁵ enables us
104 to fit this two-stage process model to choice data (Fig. 1b-d, full lines). Before doing so, we first derive a set of basic model
105 predictions.

106 **Deriving model predictions**

107 To gain a deeper understanding of the impact of the different model components on confidence reports, we investigated the
108 model's behavior in a continuous 2-AFC discrimination task with binary confidence report options ("confident" or "not confi-
109 dent"). We assumed the decision variable's mean value to be stimulus-dependent (in this simulation, it is identical to the true
110 stimulus value). All other model components were varied independently of the stimulus (see Methods). Altering the first-stage
111 decision criterion (Fig. 2a, top left, orange vs grey line) affects the confidence variable distribution by shifting its mode and,

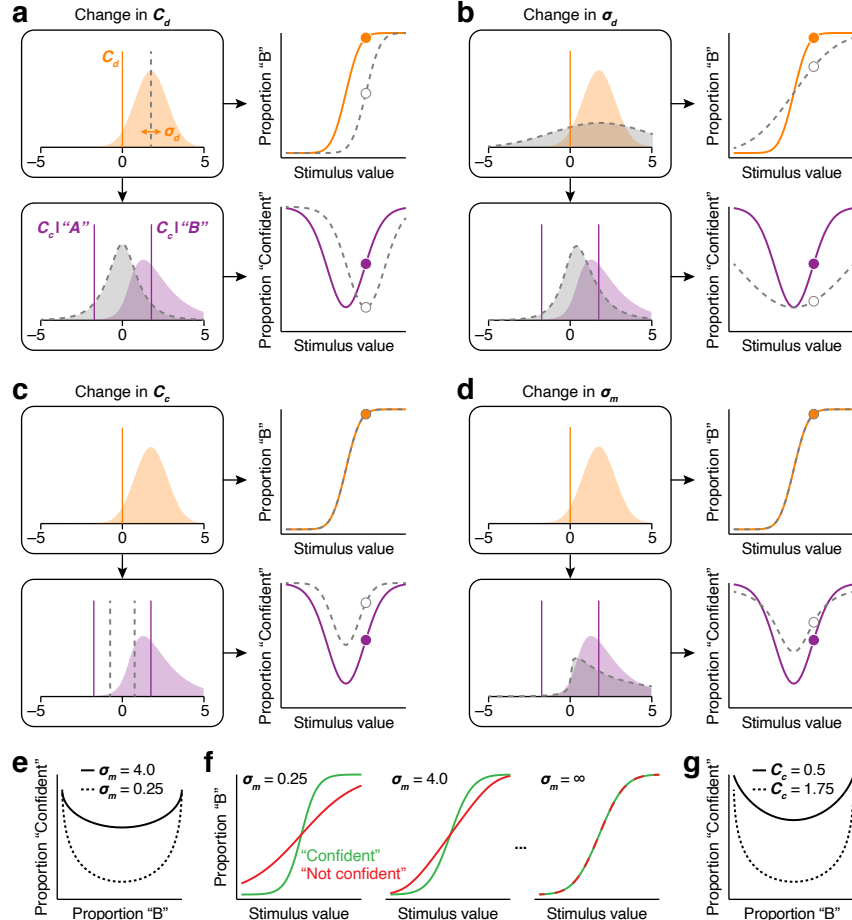


Figure 2 Impact of the different model components on primary choice behavior and confidence reports. **(a)** Top left: illustration of the decision criterion (orange line) and the decision variable distribution elicited by repeated presentations of the same stimulus (orange distribution). Bottom left: the associated confidence variable distribution (purple distribution). V_c is a positive-valued variable. As plotting convention, we reserve negative values for “Category A” choices, and positive values for “Category B” choices. The confidence criterion (purple line) therefore shows up twice in this graph. Top right: the resulting psychometric function over a range of stimulus values (orange line). The filled symbol corresponds to the condition depicted on the left hand side. Bottom right: same for the resulting confidence function. All panels: the grey dotted line illustrates how the model predictions change when a specific model component (here, the decision criterion) is altered. The open symbol corresponds to the condition depicted on the left hand side. **(b)** Increasing the level of stimulus uncertainty affects both primary decisions and confidence reports. **(c)** Lowering the confidence criterion yields more “confident” reports at all stimulus values. **(d)** Increasing meta-uncertainty increases the fraction of “confident” reports for weak stimuli, but has the opposite effect for strong stimuli. **(e)** The confidence-consistency relation for two levels of meta-uncertainty. All other model parameters held equal. **(f)** The psychometric function, split out by confidence report (“confident” in green vs “not confident” in red), for three levels of meta-uncertainty. **(g)** The confidence-consistency relation under a liberal vs a conservative confidence criterion. All other model parameters held equal, $\sigma_m = 0.25$.

in the presence of meta-uncertainty, its spread and skew (Fig. 2a, bottom left, purple vs grey distribution). At the level of observables, this manipulation results in a horizontal shift of the “psychometric function” that characterizes how choices depend on stimulus value (Fig. 2a, top right). This shift is accompanied by an identical shift of the “confidence function” that characterizes how confidence reports depend on stimulus value (Fig. 2a, bottom right). Effects of this kind have been documented for human^{20,36,37} and animal^{38,39} subjects. Altering the level of first-stage noise (Fig. 2b, top left, orange vs grey distribution) affects the confidence variable distribution by changing its mode and, in the presence of meta-uncertainty, its spread and skew (Fig. 2b, bottom left, purple vs grey distribution). At the level of choice behavior, this manipulation changes the slope of the psychometric function (Fig. 2b, top right) as well as the overall fraction of “confident” reports (Fig. 2b, bottom right). In contrast, the parameters that control the model’s second-stage operations do not affect the primary choice behavior but only the confidence reports. Specifically, changing the confidence criterion (Fig. 2c, bottom left, purple vs grey lines) mainly impacts the confidence function by shifting it vertically (Fig. 2c, bottom right). Changing the level of meta-uncertainty alters the confidence variable distribution’s mode, variance, and skew (Fig. 2d, bottom left, purple vs grey distribution), resulting in a complex pattern of changes in the confidence function (Fig. 2d, bottom right).

What does it mean to say that someone has good or bad self-knowledge? The CASANDRE model provides a principled answer that is at once intuitive and revealing. Everything held equal, increasing meta-uncertainty makes the confidence variable distribution more heavy-tailed (Fig. 2d, bottom left). This in turn leads to an increase in the fraction of “confident” reports for weak stimuli, but has the opposite effect for strong stimuli (Fig. 2d, bottom right). As a consequence, the dynamic range of the confidence-consistency relation decreases (Fig. 2e). However, these effects are not balanced. In particular, when meta-uncertainty is high, there is a dramatic increase in “confident” reports for the most difficult conditions (Fig. 2e, full black line). This increase does not reflect an actual change in task performance (Fig. 2d, top right). Rather, the association between confidence and choice consistency has weakened. This can be appreciated by inspecting the psychometric function split out by confidence report. When meta-uncertainty is low, “confident” decisions tend to be much more reliable than “not confident” decisions (Fig. 2f, left, green vs red). As meta-uncertainty increases, this distinction weakens and eventually disappears (Fig. 2f, middle-right). In sum, under the CASANDRE model, a lack of self-knowledge means having a limited capacity to distinguish reliable from unreliable decisions (note that this is not the same as distinguishing correct from incorrect decisions)²⁰. This is a practical and useful insight. However, the magnitude of the effects shown in Fig. 2e,f depends on the other model components as well (e.g., Fig. 2g). These components will rarely be constant across tasks, individuals, or the life-span. Determining the level of meta-uncertainty therefore requires directly fitting the model to data.

Evaluating the model architecture

We have motivated our framework on the basis of a qualitative observation (the lawful confidence-consistency relationship) and first principles (the inherent noisiness of perceptual and cognitive processes). To further test the central tenets of the CASANDRE model, we quantitatively examined the choice-confidence data collected by Adler and Ma (2018). We conducted several model comparisons designed to interrogate the framework’s second-stage operations. For this reason, we began by fitting the first-stage parameters to each subject’s choice data and then kept these parameters constant across all model variants (see example in Fig. 3a). We first asked whether a simpler computation can account for confidence reports. We compared a model variant in which confidence reflects a subject’s estimate of stimulus strength^{14,29–33} with one in which it reflects an estimate of decision reliability (i.e., stimulus strength normalized by stimulus uncertainty; Fig. 3b, left). To quantify model quality, we computed each model’s AIC value (see Methods). For all 19 subjects, the more complex model outperformed the simpler variant (median difference in AIC = 1179.5; Fig. 3c, top). We then asked whether meta-uncertainty is a necessary model component, and found this to be the case (Fig. 3b, middle). Including meta-uncertainty improved model quality for all 19 subjects (median difference in AIC = 285.2; Fig. 3c, middle). These model comparisons thus provide strong and consistent support for the hypothesis that confidence reflects a subject’s noisy estimate of the reliability of their decision.

Further attempts to improve the model architecture yielded comparatively weak and inconsistent results. In particular, we wondered whether model performance would benefit from allowing criterion-asymmetry (meaning that the confidence criteria depend on the primary decision) and adopting a different second-stage noise distribution (the Gamma distribution). Allowing criterion-asymmetry improved model performance for 16 out of 19 subjects (median difference in AIC = 27.9; Fig. 3b, right; Fig. 3c, bottom; different example subject shown in Supplementary Fig. 2), while the log-normal distribution was preferred over the Gamma distribution for 16 out of 19 subjects (median difference in AIC = 17.7). For simplicity, we chose to use symmetric confidence criteria for all further analyses. Finally, we compared the CASANDRE model with a model recently proposed by Shekhar and Rahnev (2021; the “criteria-noise model”). In this model, confidence reflects a subject’s estimate of evidence strength and metacognitive ability is limited by a subject’s inability to maintain constant confidence criteria across trials²⁸. As this model is tailored to experiments that employ only two levels of stimulus strength, we examined the choice-confidence data collected by Shekhar and Rahnev (2021) and found that the CASANDRE model either matched or outperformed the

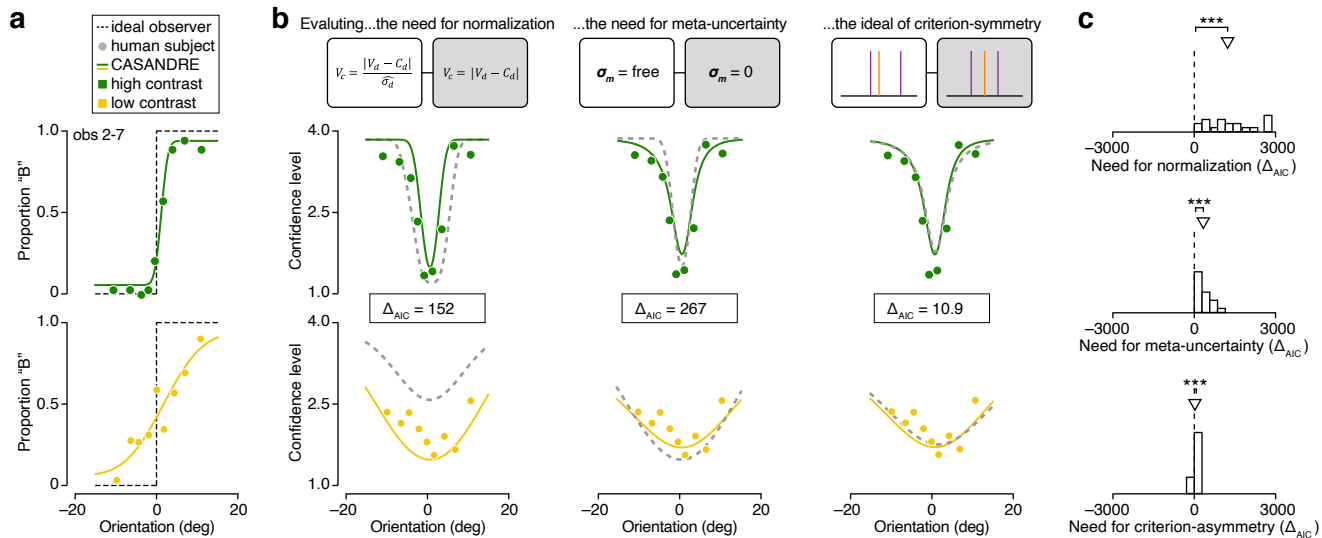


Figure 3 Comparison of different model architectures. **(a)** Proportion of "Category B" choices is plotted against stimulus orientation for high and low contrast stimuli (top vs bottom). Symbols summarize observed choice behavior of an example subject (observer 7 in experiment 2 from ref. 25), the dotted line illustrates the theoretical optimum, and the full lines show the fit of the first stage which is shared across all model variants examined in this analysis. As previously, the model was fit to all data simultaneously. **(b)** Mean confidence level is plotted as a function of stimulus orientation for the example subject. (Left) Fits of two model variants in which confidence either reflects an estimate of decision reliability (full lines) or of stimulus strength (dashed lines). (Middle) Fits of two model variants in which confidence either reflects a noisy (full lines) or noiseless (dashed lines) estimate of decision reliability. (Right) Fits of two model variants in which confidence criteria either depend (full lines) or not (dashed lines) on the primary decision. **(c)** Distribution of the difference in AIC value for each model comparison across 19 subjects. Positive values indicate evidence for the more complex model variant. Arrows indicate median of the distribution. *** $P < 0.001$, Wilcoxon signed-rank test.

165 criteria-noise model (Supplementary Fig. 8a; see Supplementary Information).

166 Estimating meta-uncertainty from sparse data

167 We seek to quantify a subject's ability to introspect about the reliability of a decision. Our method consists of interpreting human
 168 choice-confidence data through the lens of a principled two-stage process model. What kind of measurements are required to
 169 obtain robust and reliable estimates of meta-uncertainty, the model's parameter that governs metacognitive ability? We verified
 170 that Adler and Ma's experimental design affords solid parameter recovery (See Supplementary Fig. 3). However, their design
 171 is exceptional for its large number of stimulus conditions 25. Many studies use as little as two conditions 23. To test whether
 172 our approach generalizes to such experiments, we performed a recovery analysis. We used the CASANDRE model to generate
 173 synthetic data sets for five model subjects performing a 2-AFC discrimination task with binary confidence report options (see
 174 Methods). The model subjects only differed in their level of meta-uncertainty, which ranged from negligible to considerable
 175 (Fig. 4a, colored lines). We simulated data for each model subject using experimental designs that varied in the number of trials
 176 (100 vs 1,000) and in the number of conditions (2 vs 20; Fig. 4a, top). Figure 4b summarizes an example synthetic experiment.
 177 The model parameters ($\sigma_d, C_d, \sigma_m, C_c$) specify the relation between stimulus value and the probability of each response option
 178 (Fig. 4b, left). We used these probabilities to simulate a synthetic dataset of 1,000 trials distributed across 20 conditions (Fig.
 179 4b, middle). We then identified the set of parameter values that best describes these data (Fig. 4b, right). We repeated this
 180 procedure 100 times for each simulated experiment. Our method yields robust estimates of meta-uncertainty: for all model
 181 subjects and all experimental designs, the median estimate closely approximates the ground truth value (Fig. 4c, symbols). The
 182 reliability of these estimates is higher for more trials and somewhat higher for denser stimulus sampling (Fig. 4c, error bars).
 183 Estimation error in σ_m covaried with estimation error in C_c (Supplementary Fig. 7). We conclude that the CASANDRE model
 184 typically can be identified in sparse experimental designs.

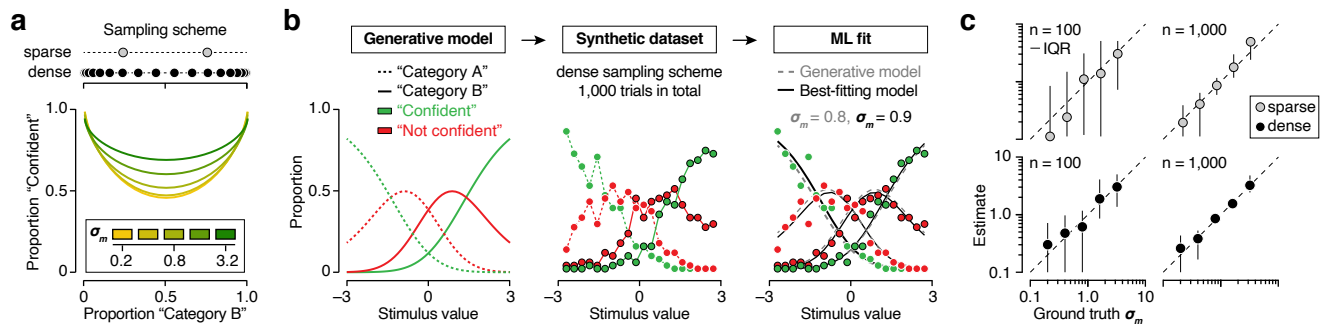


Figure 4 Model recovery analysis. (a) We simulated choice-confidence data for five model subjects who differed in their level of meta-uncertainty (colored lines) using experimental designs that varied in the number of trials (100 vs 1,000) and in the number of conditions (2 vs 20, grey and black symbols). (b) An example synthetic experiment and model-based analysis. (c) The median estimate of meta-uncertainty is plotted against the ground truth value for four experimental designs. Meta-uncertainty was limited to a minimum value of 0.1. Error bars illustrate the interquartile range (IQR) computed from 100 simulated data sets.

185 Meta-uncertainty: construct reliability and validity

186 So far, we have presented evidence that confidence is well described as reflecting a subject's decision-reliability estimate. In the
 187 CASANDRE model, the quality of this estimate is limited by meta-uncertainty. This naturally raises the question of whether
 188 meta-uncertainty is a "real" thing. In other words, do meta-uncertainty estimates isolate a stable property of human subjects
 189 that captures their metacognitive ability?

190 The most straightforward form of stability is repeatability. If we were to measure a subject's meta-uncertainty on two different
 191 occasions using the same experimental paradigm, we should obtain similar estimates. Navajas et al. (2017) conducted a
 192 perceptual confidence experiment in which 14 subjects performed the same task twice with approximately one month in between
 193 test sessions²⁴. We used the CASANDRE model to analyze their data (see Methods and Supplementary Fig. 4). Measured and
 194 predicted choice-confidence data were strongly correlated, indicating that the model describes the data well (condition-specific
 195 proportion correct choices: Spearman's rank correlation coefficient $r = 0.96$, $P < 0.001$; condition-specific mean confidence
 196 level: $r = 0.99$, $P < 0.001$). Critically, we found meta-uncertainty estimates to be strongly correlated across both sessions as
 197 well ($r = 0.78$, $P = 0.002$; Fig. 5a). This suggests that meta-uncertainty measures a stable characteristic of human confidence
 198 reporting behavior.

199 Under the CASANDRE model, meta-uncertainty provides a measure of metacognitive ability, not of confidence reporting
 200 strategy. To investigate whether this idealized pattern holds true in human choice-confidence data, we analyzed data from 43
 201 sessions where subjects either performed a perceptual or a cognitive confidence task. They reported their confidence in a binary
 202 decision using a six-point rating scale²⁴. We artificially biased these confidence reports by mapping them onto a liberal and a
 203 conservative 4-point rating scale (see Methods)⁴⁰. This manipulation resulted in a mean confidence level of 2.89 and 2.43 –
 204 a substantial difference in light of the standard deviation (the effect size, expressed as Cohen's d , is 3.16). We then used the
 205 model to analyze both perturbed versions of the data (see Methods). Meta-uncertainty estimates were strongly correlated ($r =$
 206 0.84, $P < 0.001$; Fig. 5b), though note that they were on average higher for the conservatively biased version of the data (mean
 207 increase: 47%, median increase: 0%, $P = 0.002$, Wilcoxon signed rank test). This suggests that meta-uncertainty estimates are
 208 largely, but not fully, independent of subjects' confidence reporting strategy.

209 We wondered whether meta-uncertainty depends on the absolute level of stimulus uncertainty⁴¹. We analyzed data from 43
 210 sessions where subjects either performed a perceptual or cognitive confidence task. In both tasks, stimulus uncertainty was
 211 manipulated by varying the variance of the category distributions over four levels²⁴. We used the CASANDRE model to
 212 analyze these data and estimated meta-uncertainty separately for the two lowest and the two highest levels of stimulus variance
 213 (see Methods). The former conditions resulted in a much higher task performance than the latter (average proportion correct
 214 decisions: 87% vs 70%). According to the model, the corresponding underlying levels of stimulus uncertainty, σ_d , averaged
 215 2.61 and 8.71. While increasing stimulus variance tripled stimulus uncertainty, meta-uncertainty estimates did not change
 216 much (median change: -14.76%, $P = 0.004$, Wilcoxon signed rank test). Moreover, meta-uncertainty estimates were strongly
 217 correlated across both sets of conditions ($r = 0.70$, $P < 0.001$; Fig. 5c). This suggests that meta-uncertainty is largely, but not
 218 fully, independent of the absolute level of stimulus uncertainty.

219 Whether metacognitive ability is domain-specific or domain-general is a debated question^{8,42–44}. We analyzed data from 20
 220 subjects who performed a perceptual and cognitive confidence task. Both tasks had the same experimental design. Stimulus

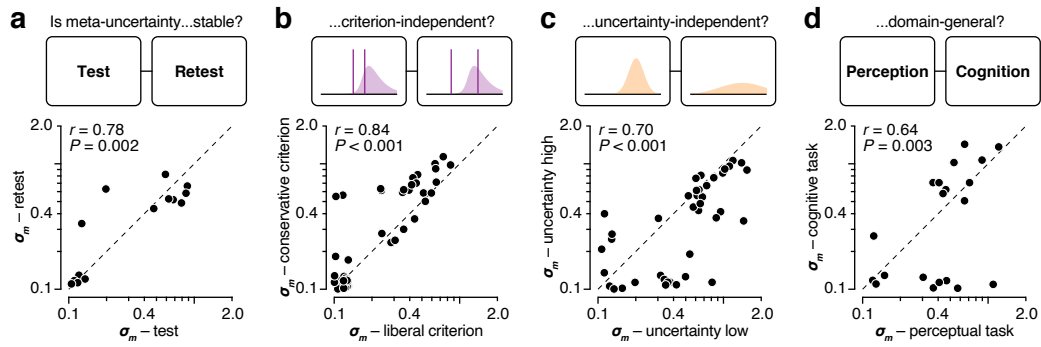


Figure 5 Evaluating meta-uncertainty as a psychological construct. **(a)** Comparison of meta-uncertainty estimates for 14 subjects who performed the same perceptual confidence task on two different occasions, separated by 1 month. We added a small amount of jitter to get a better view of overlapping data points in the lower left region of the plot. Meta-uncertainty was limited to a minimum value of 0.1. **(b)** Comparison of meta-uncertainty estimates for 43 sessions (performed by 32 subjects, see methods) whose 6-point confidence ratings were mapped onto a liberal and conservative 4-point rating scale. **(c)** Comparison of meta-uncertainty estimates for 43 sessions where subjects performed a confidence task involving low and high levels of stimulus uncertainty. **(d)** Comparison of meta-uncertainty estimates for 20 subjects who performed a perceptual and cognitive confidence task.

221 categories were either defined by the average orientation of a series of rapidly presented gratings, or by the average value
 222 of a series of rapidly presented numbers²⁴. Subjects' performance level was correlated across both tasks (condition-specific
 223 proportion correct choices: $r = 0.69, P < 0.001$), and so were their reported confidence levels, albeit to a lesser degree ($r =$
 224 $0.53, P < 0.001$). We used the CASANDRE model to analyze both data-sets (see Methods). Meta-uncertainty estimates were
 225 strongly correlated ($r = 0.64, P = 0.003$; Fig. 5d). Thus, meta-uncertainty appears to capture an aspect of confidence-reporting
 226 behavior that generalizes across at least some domains.

227 Comparison with other metrics for metacognitive ability

228 Our method to analyze choice-confidence data is built on the hypothesis that metacognitive ability is determined by meta-
 229 uncertainty. It is natural to ask how this metric of metacognitive ability relates to alternatives. We approach this question in
 230 two ways. First, by investigating this relationship in silico whilst using the CASANDRE model as generative model of choice-
 231 confidence reports. And second, by comparing performance of these different candidate-metrics on a set of real bench-marking
 232 experiments (the tests shown in Fig. 5a-d).

233 One historically popular approach to quantify metacognitive ability consists of measuring the trial-by-trial correlation between
 234 choice accuracy and the confidence report (this metric is sometimes termed "phi")¹². Consider an analysis of the choice-
 235 confidence reports of five model subjects who differed in their level of meta-uncertainty. We additionally varied the other
 236 model components in a step-wise fashion and computed phi for each simulated experiment. This analysis revealed a complex
 237 interdependence of the effects of the different model components on phi (Fig. 6a, top). An alternative method to quantify
 238 metacognitive ability that has gained popularity in recent years seeks to estimate how well confidence judgements distinguish
 239 correct from incorrect decisions^{13,45}. This estimate is expressed in signal-to-noise units and often termed "meta-d". The
 240 ratio of meta-d' and stimulus discrimination ability (d') theoretically provides a measure of metacognitive efficiency and is
 241 often considered the quantity of interest⁴⁵. Under the CASANDRE model, the meta-d'/d' metric does not provide a direct
 242 measurement of meta-uncertainty, but instead reflects a complex mixture of model components (Fig. 6a, middle).

243 Finally, a recently introduced model of confidence judgments attributes metacognitive inefficiencies to perfectly correlated
 244 cross-trial variability in the confidence criteria²⁸. For experiments involving only two levels of stimulus strength, criteria noise
 245 can be estimated by fitting this model to choice-confidence data²⁸. In a practical sense, correlated criteria noise resembles meta-
 246 uncertainty in that it solely impacts confidence reports. However, assuming noisy uncertainty estimates versus noisy confidence
 247 criteria results in metrics that behave somewhat differently (Fig. 6a, bottom).

248 Now consider the relationship between these metrics and meta-uncertainty for the three experiments performed by Navajas et al.
 249 (2017). Meta-uncertainty estimates and phi are well correlated ($r = -0.60, P < 0.001$, Spearman correlation, Fig. 6b, top). But
 250 the correlation of two other model components with phi also reaches statistical significance: stimulus uncertainty ($r = -0.59,$
 251 $P < 0.001$) and the confidence criterion ($r = -0.24, P = 0.028$). Likewise, meta-uncertainty and meta-d'/d' are well correlated
 252 ($r = -0.52, P < 0.001$, Fig. 6b, middle). But the confidence criterion is also correlated with meta-d'/d' ($r = -0.29, P = 0.008$).

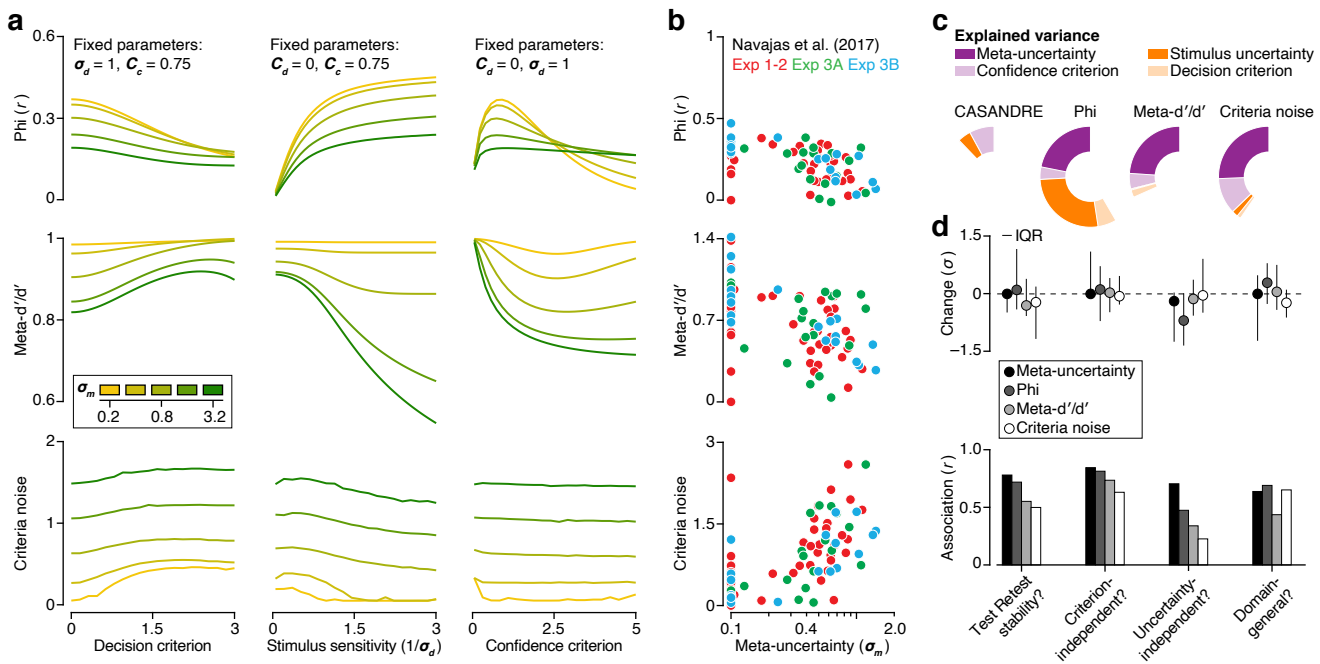


Figure 6 Comparing meta-uncertainty with three existing metrics of metacognitive ability. **(a)** We simulated choice-confidence data for a set of model observers who differed in their level of meta-uncertainty (colored lines) and additionally varied the decision criterion (left), the level of stimulus uncertainty (middle), and the confidence criterion (right). We estimated phi (top), meta- d'/d' (middle), and criteria noise (bottom) for each simulated experiment. **(b)** Phi (top), meta- d'/d' (middle), and criteria noise (bottom) plotted against meta-uncertainty estimates for three confidence experiments. Each symbol summarizes data from a single session (84 total sessions across 50 subjects, see methods). Meta-uncertainty was limited to a minimum value of 0.1. **(c)** Wedges indicate the proportion of variance in meta-uncertainty (left), phi, meta- d'/d' , and criteria noise explained by each model component. **(d)** Comparison of the performance of four metrics of metacognitive ability in four bench-marking tests. Top: analysis of estimation bias. Bottom: analysis of estimation robustness. Error bars illustrate the interquartile range (IQR) across subjects.

Finally, meta-uncertainty and criteria noise are well correlated ($r = 0.64$, $P < 0.001$, Fig. 6b, bottom). But the confidence criterion is also correlated with criteria noise ($r = 0.37$, $P < 0.001$). Variability in each of these metrics of metacognitive ability thus in part reflects variability in meta-uncertainty, and in part variability in other components of the CASANDRE model.

To identify the relative importance of the different model components, we decomposed the variance of these metrics using the averaging-over-orderings technique (see Methods)^{46,47}. We first asked whether variability in meta-uncertainty could be explained by other model components, but found this not to be the case (fraction of explained variance: 13%, Fig. 6c). In contrast, variability in phi is predominantly explained by stimulus uncertainty (27%), followed by meta-uncertainty (22%). For meta- d'/d' and criteria noise, most variance is explained by meta-uncertainty (24% and 26%) while the contribution of the other model components is rather small (Fig. 6c). In summary, for all three alternative metrics, about three quarters of the variance arises from factors other than meta-uncertainty.

Our analysis suggest that phi, meta- d'/d' , and criteria noise do not isolate the factors that limit metacognitive ability but instead measure a complex mixture of factors underlying choice-confidence data. We wondered how the performance of these mixtures in bench-marking experiments compares to that of meta-uncertainty. We computed phi, meta- d'/d' , and criteria noise for the data sets shown in Fig. 5a-d. For each test, we first asked whether the manipulation induced a systematic change in the range of the different metrics. This was generally not the case. Change, expressed in units of standard deviation, tended to be small for all four metrics (Fig. 6d, top). We then asked for each test whether the different metrics were correlated across both test conditions. Correlations ranged from weak to strong levels, with three tests failing to reach statistical significance (uncertainty independence of criteria noise: $r = 0.23$, $P = 0.145$; test-retest reliability of criteria noise: $r = 0.50$, $P = 0.072$; and domain generality of meta- d'/d' : $r = 0.44$, $P = 0.056$). Overall, meta-uncertainty compared favorably to the alternative metrics. The mean correlation value across the four tests was 0.74 for meta-uncertainty, 0.67 for phi, 0.52 for meta- d'/d' , and 0.50 for criteria noise (all correlations are shown in Fig. 6d, bottom).

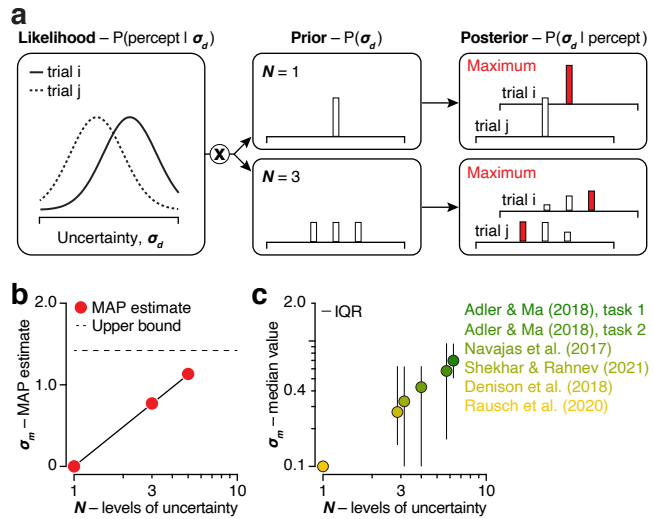


Figure 7 Meta-uncertainty depends on task structure. (a) We studied how meta-uncertainty depends on the number of uncertainty levels under an ideal Bayesian uncertainty estimation strategy. The likelihood of each uncertainty value is computed from a sensory measurement (left) while a prior belief function specifies task-specific knowledge of possible uncertainty values (middle). The product of the prior and likelihood gives the posterior (right). Due to noise, the likelihood function will differ across repeated trials (left: full vs dotted line). The impact of this variability on the posterior depends on the dispersion of the prior (right: top vs bottom panel). (b) Meta-uncertainty plotted against number of uncertainty levels for the ideal Bayesian estimator. The upper bound (dotted line) is set by the cross-trial variability of the maximum of the likelihood function and is reached when the prior is a uniform distribution. (c) Median level of meta-uncertainty plotted against number of uncertainty levels for six confidence experiments. Meta-uncertainty was limited to a minimum value of 0.1. Error bars illustrate the interquartile range (IQR) across subjects (Adler and Ma (2018) task 1: 19 subjects; task 2: 34 subjects; Navajas et al. (2017): 50 subjects; Shekhar and Rahnev (2021): 20 subjects; Denison et al. (2018): 12 subjects; Rausch et al. (2020): 25 subjects).

274 Manipulating meta-uncertainty

275 Can metacognitive ability be manipulated experimentally? Key to our framework is that confidence judgements require a subject
 276 to estimate uncertainty on a trial-by-trial basis. This becomes more difficult when experiments involve more confusable levels
 277 of stimulus uncertainty. We therefore expect that meta-uncertainty will grow with the number of stimulus uncertainty levels.
 278 To appreciate our logic, consider the ideal Bayesian uncertainty estimation strategy which consists of combining information
 279 obtained from ambiguous sensory measurements with prior task-specific knowledge. Specifically, the sensory measurement
 280 informs the uncertainty likelihood function, while knowledge of task statistics (i.e., the distribution of stimulus uncertainty
 281 levels) is summarized in a prior uncertainty belief function (Fig. 7a). The combination of both yields a posterior uncertainty
 282 belief function, the maximum of which is the "best possible" uncertainty estimate (Fig. 7a). Due to noise, repeated presentations
 283 of the same condition will yield different likelihood functions (Fig. 7a, see Methods). If the task involves only one level of
 284 stimulus uncertainty, the prior is a fixed delta function, and so is the posterior. Consequently, the maximum posterior estimate
 285 will not vary across trials and the ideal estimation strategy results in zero meta-uncertainty. However, when a task involves
 286 multiple levels of stimulus uncertainty, the prior will be more dispersed, causing the resulting maximum posterior estimate to be
 287 more variable across trials. Under an ideal Bayesian estimation strategy, meta-uncertainty thus initially grows with the number
 288 of uncertainty levels (Fig. 7b). We wondered whether this normative prediction affords insight into human metacognition.
 289 To test this hypothesis, we used the CASANDRE model to analyze six confidence experiments that varied in the number of
 290 randomly interleaved uncertainty levels (see Methods). These experiments utilized different stimuli and employed different
 291 experimental designs^{24–28}. Yet, as expected, meta-uncertainty appears to grow lawfully with the number of uncertainty levels
 292 (Fig. 7e).

293 Discussion

294 It has long been known that humans and other animals can meaningfully introspect about the quality of their decisions
 295 and actions^{5–7,31,48}. Quantifying this ability has remained a significant challenge, even for simple binary decision-making
 296 tasks^{12,13,15,28,40,41}. The core problem is that observable choice-confidence data reflect metacognitive ability as well as task

297 difficulty and response bias. To overcome this problem, we introduced a metric that is anchored in an explicit hypothesis about
298 the decision-making process that underlies behavioral reports. Our method is based on likening choice-confidence data to the
299 outcome of an abstract mathematical process in which confidence reflects a subject's noisy estimate of their choice reliability,
300 expressed in signal-to-noise units^{14,20,49}. This framework allowed us to specify the effects of factors that limit metacognitive
301 ability and to summarize this loss in a single, interpretable parameter: meta-uncertainty. We showed that this process model
302 (which we term the CASANDRE model) can explain the effects of stimulus strength and stimulus reliability on confidence
303 reports and that meta-uncertainty can be estimated from conventional experimental designs. We found that a subject's level of
304 meta-uncertainty is stable over time and across at least some domains. Meta-uncertainty can be manipulated experimentally: it
305 is higher in tasks that involve more levels of stimulus reliability. Meta-uncertainty appears to be mostly independent of task dif-
306 ficulty and confidence reporting strategy. Widely used metrics for metacognitive ability are poor proxies for meta-uncertainty.
307 As such, the CASANDRE model represents a notable advance toward realizing crucial medium and long-term goals in the field
308 of metacognition⁵⁰.

309 The mental operations underlying confidence in a decision have long intrigued psychologists. Two key unresolved issues are
310 the structure and nature of the confidence computation⁵⁰. At stake are two intertwined questions: (1) Does confidence arise
311 from a single, dual, or hierarchical process? and (2) What exactly does confidence reflect? Some authors have proposed that
312 decision outcome and confidence both arise from a single stimulus strength estimation process^{31,51–53}. Such models can explain
313 the effects of stimulus strength, but not of stimulus reliability. Others have argued in favor of a dual process in which decision
314 outcome and confidence are based on different stimulus strength estimates^{54–56,56,57}. This may be the appropriate framework
315 for cases in which subjects acquire additional task-relevant information after reporting their choice^{57–60}. For all other cases, it
316 appears overly complex. Instead, we have modeled confidence judgements as arising from a hierarchical process⁶¹. The first
317 stage determines the choice, the second stage determines confidence (Fig. 1e). We found that this model structure systematically
318 outperforms a single stage alternative (Fig. 3c, top). The structure of the computation clarifies its nature. Many previous
319 studies are built on the premise that confidence reflects a subject's assessment of decision accuracy ("What is the probability
320 that my choice is correct?"). This premise directly motivates Bayesian models of confidence^{1,25,31,62–68} and tacitly underlies
321 popular metrics of metacognitive ability^{13,20}. However, when experimental manipulations bias perceptual choices, aggregated
322 confidence reports do not track choice accuracy but choice consistency^{20,36,37}. At the single trial level, this suggests that
323 confidence reflects a subject's assessment of decision reliability ("What is the probability that I would make the same choice
324 again?", see equation 1). For an unbiased subject who is choosing between two alternatives, decision accuracy and decision
325 reliability are indistinguishable^{20,67}. Yet, the distinction matters greatly, as it implies that the same computation that underlies
326 confidence in decisions with a well-defined correct and incorrect option may generalize to subjective domains that lack this
327 feature ("Which political candidate will I support?", "Which beer will I have?", "Should I skip class today?").⁶⁹

328 Key to our proposal is that assessing the reliability of a decision requires the use of additional information (stimulus un-
329 certainty)²¹ that in most tasks has no relevance for the choice as such. The notion that subjects can incorporate a stimulus
330 uncertainty estimate when making perceptual inferences is well established^{25,70–72}. And there is considerable evidence that
331 neural activity in sensory areas of the brain conveys information about stimulus features as well as the uncertainty of those
332 features^{68,73–78}. Our proposed confidence computation yielded a new prediction: the more levels of stimulus uncertainty a task
333 involves, the more variable uncertainty estimates will be. We validated this prediction by analyzing data from six different con-
334 fidence experiments in which 160 subjects completed a total of 243,000 trials (Fig. 7c). This finding is arguably the strongest
335 piece of empirical evidence that meta-uncertainty is the critical factor that limits human metacognitive ability. It was enabled
336 by the use of modern computational tools to quickly compute the approximate ratio of two distributions (i.e., the confidence
337 variable distribution) and by the availability of the confidence database²³. This phenomenon also raises the question to what
338 degree metacognitive ability estimates are influenced by experimental design. For example, studies that increase the volatility
339 of stimuli within a trial (thereby making uncertainty more difficult to estimate) report confidence distortions that could likely
340 be captured by the CASANDRE model^{79–81}. An important future direction will be to investigate the effect of different stimulus
341 uncertainty distributions on metacognitive ability.

342 The CASANDRE model provides a static description of the outcome of a hierarchical decision-making process. However,
343 making a decision requires time. The more difficult the decision, the more time it requires^{82,83}. For this reason, some authors
344 have suggested that decision time directly informs confidence^{58,84}. This proposal enjoys strong empirical support^{38,63,80,84}. It
345 is related to our proposed confidence computation, provided that the decision variable results from a mechanism that resembles
346 bounded evidence accumulation⁷. For these mechanisms, time to reach the bound reflects the drift rate of a drift diffusion
347 process. Drift rate is governed by stimulus strength, normalized by stimulus uncertainty and thus determines decision reliability.
348 Moreover, just like our second stage involves an additional factor to reflect on the quality of the decision (the uncertainty
349 estimate), time measurements are not inherent to bounded accumulation. Like uncertainty estimates, neural and behavioral
350 time measurements are strictly positive and noisy^{85–87}. This noisiness provides the conceptual dynamic analogue for meta-

351 uncertainty in our static model. How it affects confidence reporting behavior in the diffusion-to-bound framework has not
352 yet been studied. It remains to be seen whether choice outcome, reaction time, and metacognitive ability can all be modeled
353 simultaneously.

354 Process models are powerful tools to study cognition and perception. Here we leveraged a process model to interrogate the
355 computations underlying our sense of confidence, to determine the effectiveness of various experimental designs, and to examine
356 model recoverability. However, the usefulness of process models far exceeds our current application. Specifically, when
357 coupled to an explicit goal such as maximizing choice accuracy, process models can be used to derive the optimal task strategy.
358 The resulting predictions offer a critical point of reference for human behavior⁸⁸. This approach has revealed that humans
359 improve the quality of uncertain decisions by accumulating evidence over time⁸², by combining information acquired through
360 different sensory modalities⁷⁰, and by exploiting knowledge of statistical regularities in the environment⁸⁹. Might the same
361 hold true for uncertain confidence judgments? Stated more generally: Does our brain attempt to maximize the precision of our
362 sense of confidence? This is a fundamental question that is ripe to be addressed. Doing so will require experiments that ma-
363 nipulate meta-uncertainty and incentivize the confidence reporting strategy (e.g., refs.^{31,48,53,55,63,90-92}). The process model we
364 have developed provides a vehicle to derive the reward-maximizing strategy and to evaluate whether human meta-uncertainty
365 changes as expected for theoretically ideal introspection. We took a first step in this direction and validated a novel prediction:
366 meta-uncertainty changes with task-structure as expected under an ideal Bayesian uncertainty estimation strategy.

367 Methods

368 Modeling: Hierarchical decision-making process

369 We model choice-confidence data in binary decision-making tasks as arising from a hierarchical process. The first stage follows
370 conventional signal detection theory applications²² and describes the primary decision as resulting from the comparison of a
371 one-dimensional decision variable, V_d , with a fixed criterion, C_d . The decision variable is subject to zero-mean Gaussian noise
372 and hence follows a normal distribution with mean μ_d and standard deviation σ_d . The decision variable is converted into a
373 signed confidence variable, V'_c , by taking the difference of V_d and C_d , and dividing this difference by $\hat{\sigma}_d$, the subject's estimate
374 of σ_d . The family of normal distributions is closed under linear transformations. This means that, if $\hat{\sigma}_d$ were a constant, V'_c
375 would also follow a normal distribution with mean $\mu'_c = (\mu_d - C_d)/\hat{\sigma}_d$ and standard deviation $\sigma'_c = \sigma_d/\hat{\sigma}_d$. The confidence
376 report results from the comparison of the confidence variable with a single fixed criterion, C_c (or with a set of criteria if the
377 confidence scale has more than two levels). It follows that the probability of a “confident” judgement given a “Category A”
378 decision is given by $P(C = 1|D = 0) = \Phi(-C_c)$, where $\Phi(\cdot)$ is the cumulative normal distribution with mean μ'_c and
379 standard deviation σ'_c . By the same logic, $P(C = 0|D = 0) = \Phi(0) - \Phi(-C_c)$, $P(C = 0|D = 1) = \Phi(C_c) - \Phi(0)$, and
380 $P(C = 1|D = 1) = 1 - \Phi(C_c)$. Key to the CASANDRE model is that $\hat{\sigma}_d$ is not a constant, but a random variable that follows
381 a log-normal distribution with mean σ_d and standard deviation σ_m . Consequently, the signed confidence variable is a mixture
382 of normal distributions, with mixing weights determined by σ_m . To obtain the probability of each response option under this
383 mixture, we sample $\hat{\sigma}_d$ in steps of constant cumulative density (using the Matlab function ‘logninv’), compute the probability
384 of each response option under each sample’s resulting normal distribution (using the Matlab function ‘normcdf’), and average
385 these probabilities across all samples. We found that this procedure yields stable probability estimates once the number of
386 samples exceeds 25 (i.e., sampling the log-normal distribution in steps no greater than 4%). For all applications in this paper,
387 we used 100 samples, thus sampling $\hat{\sigma}_d$ at a cumulative density of 0.5%, 1.5%, 2.5%,..., and 99.5%. Finally, note that whenever
388 we report values for σ_m , we use the coefficient of variation (σ_m/σ_d), as this ratio is identifiable under the model (the absolute
389 level of meta-uncertainty is not, just like the absolute level of σ_d cannot be uniquely estimated from choice data).

390 Modeling: Parameterization, simulations, and fitting

391 We analyzed data from a large set of previously published studies that employed different task designs. The simplest designs
392 involve the combination of a 2-AFC categorization decision and a binary confidence report (i.e. the model simulations shown
393 in Fig. 2 and 4). Under the CASANDRE model, the predicted probability of each response option is fully specified by five
394 parameters: the mean of the decision variable (μ_d), the standard deviation of the decision variable (σ_d), the decision criterion
395 (C_d), the level of meta-uncertainty (σ_m), and the confidence criterion (C_c). It is not possible to estimate each of these parameters
396 for every unique experimental condition. To make the model identifiable, we generally assume that μ_d is identical to the true
397 stimulus value, that σ_d is constant for a given level of stimulus reliability, and that C_d , σ_m and C_c are constant across multiple
398 conditions. We limited σ_m to a minimum value of 0.1, as values below this had indistinguishable effects on model behavior.
399 Figure 2 shows how each of the parameters affects the model’s behavior. Finally, when fitting data, we use one additional
400 parameter, λ , to account for stimulus-independent lapses⁹³, which we assume to be uniformly distributed across all response
401 options. We fit the model on a subject-by-subject basis. For each subject, we compute the log-likelihood of a given set of model

402 parameters across all choice-confidence reports and use an iterative procedure to identify the most likely set of parameter values
403 (specifically, the interior point algorithm used by the Matlab function ‘fmincon’). Figure 4b shows an example model fit to a
404 synthetic data set whereby we used 5 free parameters (λ , σ_d , C_d , σ_m , and C_c) to capture data across 20 experimental conditions.

405 Some studies used a task design that combined a 2-AFC categorization decision with a multi-level confidence rating scale (i.e.,
406 ref. [24,25,27,28](#)). To model these data, we used the same approach as described above but we used multiple confidence criteria
407 (one less than the number of confidence levels). We modeled the data from ref. [27](#) using seven free parameters: λ , σ_d , C_d , σ_m ,
408 and C_c (4-point confidence rating scale, thus three in total) (see Fig. 7c and Supplementary Fig. 5a). We modeled some data
409 from ref. [25](#) (task 1) using seventeen free parameters: λ , σ_d (one per contrast level, six in total), C_d (one per contrast level,
410 six in total), σ_m , and C_c (4-point confidence rating scale, thus three in total). Example fits are shown in Fig. 1b,c and in
411 Supplementary Fig. 1 (also see Fig. 7c, task 1 and Supplementary Fig. 5e). We modeled the data from ref. [24](#) using twelve free
412 parameters: λ , σ_d (one per stimulus variance level, four in total), C_d , σ_m , and C_c (6-point confidence rating scale, thus five in
413 total). Example fits are shown in Supplementary Fig. 4 (also see Fig. 7c, Fig. 6b-d, and Supplementary Fig. 5d). We modeled
414 the data from ref. [28](#) using 10 free parameters: σ_d (one per stimulus reliability level, three in total), C_d , σ_m , and C_c (continuous
415 confidence rating scale, discretized into 6-point confidence rating scale, thus five in total). See Fig. 7c, and Supplementary Fig.
416 5b).

417 Some studies used a task design in which the 2-AFC categorization decision pertained to two category distributions with
418 the same mean but different spread (i.e., ref. [25,26](#)). To model these data, we assumed that the primary decision results from
419 a comparison of the decision variable with two decision criteria, and that the confidence estimate is based on the distance
420 between the decision variable and the nearest decision criterion. We modeled some data from ref. [25](#) (task 2) using twenty-three
421 free parameters: λ , σ_d (one per contrast level, six in total), C_d (two per contrast level, twelve in total), σ_m , and C_c (4-point
422 confidence rating scale, thus three in total). See Fig. 7c, task 2. Example fits are shown in Supplementary Fig. 6 (also see
423 Supplementary Fig. 5e). We modeled data from ref. [26](#) using twenty-two free parameters: λ , σ_d (one per attention level, three
424 in total), C_d (two per attention level, six in total), σ_m (one per attention level, three in total), and C_c (4-point confidence rating
425 scale, one set per attention level, thus nine in total). See Fig. 7c and Supplementary Fig. 5c.

426 Some studies used a task design that combined a 2-IFC categorization decision with a confidence report (i.e., Arbuzova and
427 Filevich, unpublished but available in the Confidence Database [23](#)). In these tasks, a subject is shown two stimulus intervals
428 and judges which interval contained the “signal” stimulus. To model such data, we assume that the decision is based on
429 a comparison of the evidence provided by each stimulus interval. The one-dimensional decision variable, V_d , reflects the
430 outcome of this comparison, which we model as a difference operation [22](#). The difference of two Gaussian distributions is itself
431 a Gaussian with mean equal to the difference of the means and standard deviation equal to the square root of the sum of the
432 variances. Everything else is the same as for the 2-AFC task. When different from zero, C_d now reflects an interval bias (e.g.,
433 a preference for “interval 1” choices). See example fit in Fig. 1d.

434 Modeling: Model comparison

435 We evaluated CASANDRE’s assumed confidence computation and overall model architecture by fitting different model variants
436 to an experiment that involved joint manipulations of stimulus strength and stimulus reliability (ref. [25](#), task 1, 19 subjects). For
437 each model comparison, we computed the Akaike Information Criterion, given by:

438
$$AIC = -2\ln(L) + 2k,$$

439 where L is the maximum value of a model’s likelihood function and k is the number of fitted parameters. To focus this analysis
440 on the model’s second-stage operations, we began by fitting 13 first-stage parameters to each subject’s choice data: λ , σ_d
441 (one per contrast level, six in total), C_d (one per contrast level, six in total). These parameters were kept constant across all
442 model variants. The head-to-head model comparisons consisted of (1) confidence as a noiseless stimulus strength estimate vs
443 confidence as a noiseless decision reliability estimate, (2) confidence as a noiseless decision reliability estimate vs confidence as
444 a noisy decision reliability estimate, (3) symmetric confidence criteria vs asymmetric confidence criteria, and (4) a log-normal
445 vs Gamma second-stage noise distribution.

446 Datasets

447 The majority of our analyses focus on two studies [24,25](#). To test the effect of task structure on meta-uncertainty, we additionally
448 analyzed data from three other studies [26-28](#). The data from Navajas et al. (2017) were provided by an author [24](#). All other datasets
449 were obtained from the Confidence Database [23](#) (available at: <https://osf.io/s46pr/>). Given that the CASANDRE model
450 yields more reliable parameter estimates for longer experiments with more stimulus conditions (error bars in Fig. 4c), we
451 included all experiments from the database that involved a large number of subjects, several hundred trials per subject, and

452 multiple levels of stimulus strength and/or stimulus reliability. All detailed experimental designs and procedures are available
453 in the original publications or in abbreviated form in the Confidence Database. We briefly describe each data set below.

454 We analyzed data from all three experiments in ref.²⁵. All subjects in experiments 1 and 2 performed both task 1 (discriminating
455 categories of orientation distributions with different means but the same standard deviation; their “Task A”) and task 2
456 (discriminating categories of orientation distributions with the same mean but different standard deviations; their “Task B”).
457 Since stimulus orientations were drawn from a continuous distribution, to plot the data we grouped nearby orientations into
458 9 bins with similar numbers of trials. Data and model fits from two example subjects performing task 1 in experiment 1 are
459 shown in Fig. 1b-c and Supplementary Fig. 1. Fitted parameters from all 19 subjects who performed experiments 1 and 2 are
460 included in Fig. 7c (task 1) and Supplementary Fig. 5f. Subjects in experiment 3 performed only task 2. Data and model fits
461 from an example subject performing task 2 in experiment 3 are shown in Supplementary Fig. 6. Fitted parameters from all 34
462 subjects who performed task 2 in experiments 1, 2, and 3 are included in Fig. 7c (task 2) and Supplementary Fig. 5e.

463 We analyzed data from all 3 experiments in ref.²⁴. 30 subjects performed experiment 1. 14 of those 30 subjects returned about
464 a month after their first session to perform the same task again as experiment 2. Finally, 20 subjects performed experiment
465 3, participating in a perceptual (experiment 3A) and cognitive (experiment 3B) task in two different sessions. We analyzed
466 each of these 84 different experimental sessions independently. Data and model fits from an example subject are shown in
467 Supplementary Fig. 4. Fitted parameters and alternative metacognitive metrics from all 14 subjects who performed both
468 experiments 1 and 2 are included in Fig. 5a and Fig. 6d (Test-retest stability). Fitted parameters and alternative metacognitive
469 metrics from all 20 subjects who performed experiment 3 are included in Fig. 5d and Fig. 6d (Domain generality). Fitted
470 parameters from 50 subjects performing experiment 1 and the perceptual task of experiment 3 (experiment 3A) are included
471 in Fig. 7c and Supplementary Fig. 5d. Further analyses using these data to test the independence of meta-uncertainty from
472 confidence reporting strategy and uncertainty are explained in the next section.

473 We analyzed unpublished data from Arbuzova and Filevich (available in the Confidence Database under the name Arbuzova_474 _unpub_1)²³. This experiment demonstrates the generalization of the CASANDRE model to a visuomotor estimation
475 task as well as 2-IFC experimental designs. Data and model fits from a representative subject are shown in Fig. 1d.

476 Fitted parameters from all 25 subjects from ref.²⁷ and from all 20 subjects from ref²⁸ are included in Fig. 7c. We analyzed data
477 from 12 subjects performing a version of task 2 in ref.²⁵ with an added attention manipulation from ref.²⁶. To get the single
478 estimate of meta-uncertainty included in Fig. 7c for each subject, we averaged the values estimated from all three attention
479 conditions, as these were not significantly different.

480 Construct validity analyses

481 To test the independence between confidence reporting strategy and measures of metacognitive ability, we manipulated the
482 confidence reporting behavior of subjects across all sessions from ref.²⁴ (following an analysis developed by ref.⁴⁰). In these
483 experiments, confidence reports were measured using a six-point rating scale. We remapped responses into a four point rating
484 scale using two different grouping rules (one conservative, one liberal). The conservative mapping is [1|2 3 4|5|6], the liberal
485 mapping is [1|2|3 4 5|6] (i.e., for the conservative mapping, ratings 2, 3 and 4 were combined, and for the liberal mapping,
486 ratings 3, 4, and 5 were combined.) To limit the model comparison to the second stage of the decision making process, the
487 lapse rate, stimulus sensitivity, and perceptual criterion were shared across both model variants. Only the meta-uncertainty
488 and confidence criteria differed across both model variants. To obtain adequately constrained and stable model fits to these
489 manipulated data, we only included a session in the analysis if at least 10 responses were recorded at the highest level of the
490 confidence scale. This reduced a total of 84 sessions to 43 (and 50 subjects to 32), shown in Fig. 5b.

491 To test the independence between stimulus uncertainty and measures of metacognitive ability, we split experimental data from
492 each session in half²⁴. We estimated meta-uncertainty independently for the two easiest and the two hardest stimulus conditions.
493 To limit the model comparison to the question of whether meta-uncertainty is independent of stimulus reliability, all other model
494 parameters were fixed across conditions. For consistency with the criterion analysis, we applied the same inclusion criteria,
495 yielding data from 43 sessions included in Fig. 5c.

496 Calculating alternative metacognitive metrics

497 We probed the relation between meta-uncertainty and three alternative metrics of metacognitive ability under the CASANDRE
498 model. We used two distinct procedures for this. First, to obtain estimates of “meta- d' ”, we used the CASANDRE model
499 to specify the probability of each response option in a 2-AFC discrimination task with binary confidence report options for
500 an experiment that included two stimulus conditions. We calculated meta- d' following ref.⁴⁵. Briefly, we searched for the
501 level of sensory noise and the confidence criterion that best explained the distribution of confidence reports conditioned on the

502 primary choice, assuming a normally distributed confidence variable. The ratio of the ground truth sensory noise level and this
503 estimate is plotted in the middle panels of Fig. 6a. Second, to obtain the expected value of phi, we simulated 200,000 trials in
504 an experiment that included 20 levels of stimulus strength. We then calculated the Pearson correlation between the resulting
505 choice accuracy and confidence vectors (Fig 6a, top panels). We used these same simulated trials to fit the criteria-noise model
506 of Shekhar and Rahnev²⁸. We downloaded their parameter optimization code and modified it as appropriate to fit our simulated
507 data (available at <https://osf.io/s8fnb/>). In their procedure, a nested two-step, coarse-to-fine search algorithm is used
508 to optimize the estimated confidence criteria and the confidence criteria noise level. The resulting criteria noise estimates are
509 plotted in the bottom panels of Fig 6a. The non-smooth appearance of the curves is a consequence of instabilities in the fitting
510 procedure.

511 We also computed these alternative metrics for each session from ref.²⁴ (see Fig. 6b-d). As is conventional, we estimated d'
512 for each stimulus condition from the observed hit and false alarm rates²². To obtain estimates of “meta- d' ”, we searched for
513 the decision criterion, the set of confidence criteria, and the level of sensory noise that best explained the choice-conditioned
514 data, assuming a normally distributed confidence variable. To obtain a single meta- d'/d' estimate per session, we computed the
515 arithmetic mean across the four stimulus conditions. We computed phi for each session by calculating the Pearson correlation
516 between choice accuracy and raw confidence report. We again used the fitting procedure of Shekhar and Rahnev²⁸, estimating
517 decision criterion and four values of d' and optimizing four sets of confidence criteria and the value of criteria noise across the
518 four stimulus conditions (Fig. 6b-d).

519 To compute the proportion of variance in each alternative metric across 84 sessions²⁴ explained by different components of
520 the CASANDRE model, we used the averaging-over-orderings technique^{46,47}. We used multiple linear regression to obtain
521 the variance in a metric explained by the CASANDRE model. Then, for each model parameter we compute the difference in
522 explained variance when the parameter is included and when it is not. The resulting estimates of explained variance for each
523 parameter are plotted in Fig. 6c.

524 Bayesian uncertainty estimation

525 We examined a simple model of Bayesian uncertainty estimation (Fig. 7a-b.). We modeled the uncertainty likelihood function
526 as a Gaussian function with a mean value, μ_u , that varied from trial-to-trial. Each trial, μ_u was randomly drawn from a Gaussian
527 distribution whose average matched the true level of stimulus uncertainty, S_u , and with standard deviation σ_u . As is typical for
528 a well-calibrated model, the spread of the likelihood function equalled σ_u . We assumed three different experimental designs
529 that yielded a prior uncertainty belief function composed of a single delta function ($N = 1$), three delta functions ($N = 3$), and
530 five delta functions ($N = 5$). We simulated 1000 trials per design. In this simulation, we computed the posterior on a single
531 trial basis and selected its maximum as the MAP uncertainty estimate. Fig 7b summarizes a simulation in which $S_u = 2.5$,
532 $\sigma_u = 1.5$, and the prior belief function peaked at 2.5 for $N = 1$, at 1.67, 2.5, and 3.33 for $N = 3$, and at 0.83, 1.67, 2.5, 3.33, and
533 4.17 for $N = 5$.

534 Data availability

535 This study generated no new data. The data used in this study are available from the Confidence Database (available at:
536 <https://osf.io/s46pr/>).

537 Code availability

538 The code supporting the findings of this study and a software package implementing the CASANDRE model is publicly
539 available (<https://github.com/gorislab/CASANDRE.git>).

540 References

- 541 1. Florent Meyniel, Mariano Sigman, and Zachary F. Mainen. Confidence as Bayesian Probability: From Neural Origins to
542 Behavior. *Neuron*, 88(1):78–92, October 2015.
- 543 2. Jan Drugowitsch, André G. Mendonça, Zachary F. Mainen, and Alexandre Pouget. Learning optimal decisions with confi-
544 dence. *Proceedings of the National Academy of Sciences*, 116(49):24872–24880, December 2019.
- 545 3. Braden A. Purcell and Roozbeh Kiani. Hierarchical decision processes that operate over distinct timescales underlie choice
546 and changes in strategy. *Proceedings of the National Academy of Sciences*, 113(31):E4531–E4540, August 2016.
- 547 4. Bahador Bahrami, Karsten Olsen, Peter E. Latham, Andreas Roepstorff, Geraint Rees, and Chris D. Frith. Optimally Inter-
548 acting Minds. *Science*, 329(5995):1081–1085, August 2010.
- 549 5. Charles Sanders Peirce and Joseph Jastrow. On small differences in sensation. *Memoirs of the National Academy of*

550 *Sciences*, 3, 1884.

551 6. Roger Ratcliff. A theory of memory retrieval. *Psychological Review*, 85(2):59–108, 1978.

552 7. Douglas Vickers. *Decision processes in visual perception*. Academic Press, New York, 1979.

553 8. Vincent de Gardelle, François Le Corre, and Pascal Mamassian. Confidence as a Common Currency between Vision and

554 Audition. *PLOS ONE*, 11(1):e0147901, January 2016.

555 9. Stephen M. Fleming, Rimona S. Weil, Zoltan Nagy, Raymond J. Dolan, and Geraint Rees. Relating Introspective Accuracy

556 to Individual Differences in Brain Structure. *Science*, 329(5998):1541–1543, September 2010.

557 10. Marion Rouault, Tricia Seow, Claire M. Gillan, and Stephen M. Fleming. Psychiatric Symptom Dimensions Are Associated

558 With Dissociable Shifts in Metacognition but Not Task Performance. *Biological Psychiatry*, 84(6):443–451, September 2018.

559 11. Deanna Kuhn. Theory of mind, metacognition, and reasoning: A life-span perspective. In *Children's reasoning and the*

560 *mind*, pages 301–326. Psychology Press, 2000.

561 12. Thomas O. Nelson. A comparison of current measures of the accuracy of feeling-of-knowing predictions. *Psychological*

562 *Bulletin*, 95(1):109–133, 1984.

563 13. Stephen M. Fleming and Hakwan C. Lau. How to measure metacognition. *Frontiers in Human Neuroscience*, 8:443, 2014.

564 14. Pascal Mamassian. Visual Confidence. *Annual Review of Vision Science*, 2(1):459–481, 2016.

565 15. Matthias Guggenmos. Measuring metacognitive performance: type 1 performance dependence and test-retest reliability. *Neuroscience of Consciousness*, 2021(1):niab040, December 2021.

566 16. L. Festinger. Studies in decision: I. Decision-time, relative frequency of judgment and subjective confidence as related to

567 physical stimulus difference. *Journal of Experimental Psychology*, 32(4):291–306, 1943.

568 17. Jinoos Hosseini and William R. Ferrell. Detectability of correctness: A measure of knowing that one knows. *Instructional*

569 *Science*, 11(2):113–127, August 1982.

570 18. Thomas S. Critchfield. Signal-Detection Properties of Verbal Self-Reports. *Journal of the Experimental Analysis of Behavior*,

571 60(3):495–514, 1993.

572 19. Susan J. Galvin, John V. Podd, Vit Drga, and John Whitmore. Type 2 tasks in the theory of signal detectability: Discrimination

573 between correct and incorrect decisions. *Psychonomic Bulletin & Review*, 10(4):843–876, December 2003.

574 20. Baptiste Caziot and Pascal Mamassian. Perceptual confidence judgments reflect self-consistency. *Journal of Vision*,

575 21(12):8, November 2021.

576 21. A. Pouget, J. Drugowitsch, and A. Kepecs. Confidence and certainty: distinct probabilistic quantities for different goals. *Nature neuroscience*, 19(3):366–374, 2016.

577 22. David Marvin Green and John A. Swets. *Signal detection theory and psychophysics*, volume 1. Wiley New York, 1966.

578 23. Dobromir Rahnev, Kobe Desender, Alan L. F. Lee, William T. Adler, David Aguilar-Lleyda, Başak Akdoğan, Polina Arbuzova,

579 Lauren Y. Atlas, Fuat Balcı, Ji Won Bang, Indrit Bègue, Damian P. Birney, Timothy F. Brady, Joshua Calder-Travis, Andrey

580 Chetverikov, Torin K. Clark, Karen Davranche, Rachel N. Denison, Troy C. Dildine, Kit S. Double, Yalçın A. Duyan, Nathan

581 Faivre, Kaitlyn Fallow, Elisa Filevich, Thibault Gajdos, Regan M. Gallagher, Vincent de Gardelle, Sabina Gherman, Nadia

582 Haddara, Marine Hainguierlot, Tzu-Yu Hsu, Xiao Hu, Iñaki Iturrate, Matt Jaquière, Justin Kantner, Marcin Koculak, Mahiko

583 Konishi, Christina Koß, Peter D. Kvam, Sze Chai Kwok, Maël Lebreton, Karolina M. Lempert, Chien Ming Lo, Liang Luo, Brian

584 Maniscalco, Antonio Martin, Sébastien Massoni, Julian Matthews, Audrey Mazancieux, Daniel M. Merfeld, Denis O'Hora,

585 Eleanor R. Palser, Borysław Paulewicz, Michael Pereira, Caroline Peters, Marios G. Philiastides, Gerit Pfuhl, Fernanda

586 Prieto, Manuel Rausch, Samuel Recht, Gabriel Reyes, Marion Rouault, Jérôme Sackur, Saeedeh Sadeghi, Jason Samaha,

587 Tricia X. F. Seow, Medha Shekhar, Maxine T. Sherman, Marta Siedlecka, Zuzanna Skóra, Chen Song, David Soto, Sai Sun,

588 Jeroen J. A. van Boxtel, Shuo Wang, Christoph T. Weidemann, Gabriel Weindel, Michał Wierzchoń, Xinming Xu, Qun Ye,

589 Jiwon Yeon, Futing Zou, and Ariel Zylberberg. The Confidence Database. *Nature Human Behaviour*, 4(3):317–325, March

590 2020.

591 24. Joaquin Navajas, Chandni Hindocha, Hebah Foda, Mehdi Keramati, Peter E. Latham, and Bahador Bahrami. The idiosyncratic

592 nature of confidence. *Nature Human Behaviour*, 1(11):810–818, November 2017.

593 25. William T. Adler and Wei Ji Ma. Comparing Bayesian and non-Bayesian accounts of human confidence reports. *PLOS*

594 *Computational Biology*, 14(11):e1006572, November 2018.

595 26. Rachel N. Denison, William T. Adler, Marisa Carrasco, and Wei Ji Ma. Humans incorporate attention-dependent uncertainty

596 into perceptual decisions and confidence. *Proceedings of the National Academy of Sciences*, 115(43):11090–11095,

597 October 2018.

598 27. Manuel Rausch, Michael Zehetleitner, Marco Steinhauser, and Martin E. Maier. Cognitive modelling reveals distinct electro-

599 physiologically markers of decision confidence and error monitoring. *NeuroImage*, 218:116963, September 2020.

600 28. Medha Shekhar and Dobromir Rahnev. The nature of metacognitive inefficiency in perceptual decision making. *Psychological*

601 *Review*, 128(1):45–70, 2021.

602 29. J. D. Balakrishnan and Roger Ratcliff. Testing models of decision making using confidence ratings in classification. *Journal*

603 *of Experimental Psychology: Human Perception and Performance*, 22(3):615–633, 1996.

604 30. William R. Ferrell. A model for realism of confidence judgments: Implications for underconfidence in sensory discrimination. *Perception & Psychophysics*, 57(2):246–254, January 1995.

605 31. Adam Kepecs, Naoshige Uchida, Hatim A. Zariwala, and Zachary F. Mainen. Neural correlates, computation and behavioural

606 impact of decision confidence. *Nature*, 455(7210):227–231, September 2008.

610 32. Michel Treisman and Andrew Faulkner. The setting and maintenance of criteria representing levels of confidence. *Journal*
611 *of Experimental Psychology: Human Perception and Performance*, 10(1):119–139, 1984.

612 33. Thomas S. Wallsten and Claudia González-Vallejo. Statement verification: A stochastic model of judgment and response.
613 *Psychological Review*, 101(3):490–504, 1994.

614 34. E. T. Jaynes. Information Theory and Statistical Mechanics. *Physical Review*, 106(4):620–630, May 1957.

615 35. Sanjoy Mahajan. *Street-Fighting Mathematics: The Art of Educated Guessing and Opportunistic Problem Solving*. The MIT
616 Press, 2010.

617 36. Shannon M. Locke, Elon Gaffin-Cahn, Nadia Hosseiniavzeh, Pascal Mamassian, and Michael S. Landy. Priors and payoffs
618 in confidence judgments. *Attention, Perception, & Psychophysics*, 82(6):3158–3175, August 2020.

619 37. Andra Mihali, Marianne Broeker, and Guillermo Horga. Insightful inference compensates for distorted perception. *bioRxiv*,
620 page 2021.11.13.468497, November 2021. Type: article.

621 38. Christopher R. Fetsch, Roozbeh Kiani, William T. Newsome, and Michael N. Shadlen. Effects of cortical microstimulation on
622 confidence in a perceptual decision. *Neuron*, 83(4):797–804, 2014.

623 39. Christopher R Fetsch, Naomi N Odean, Danique Jeurissen, Yasmine El-Shamayleh, Gregory D Horwitz, and Michael N
624 Shadlen. Focal optogenetic suppression in macaque area MT biases direction discrimination and decision confidence, but
625 only transiently. *eLife*, 7:e36523, July 2018.

626 40. Kai Xue, Medha Shekhar, and Dobromir Rahnev. Examining the robustness of the relationship between metacognitive
627 efficiency and metacognitive bias. *Consciousness and Cognition*, 95:103196, October 2021.

628 41. Ji Won Bang, Medha Shekhar, and Dobromir Rahnev. Sensory noise increases metacognitive efficiency. *Journal of Experi-
629 mental Psychology. General*, 148(3):437–452, March 2019.

630 42. Li Yan McCurdy, Brian Maniscalco, Janet Metcalfe, Ka Yuet Liu, Floris P. de Lange, and Hakwan Lau. Anatomical Coupling
631 between Distinct Metacognitive Systems for Memory and Visual Perception. *Journal of Neuroscience*, 33(5):1897–1906,
632 January 2013.

633 43. Benjamin Baird, Matthew Cieslak, Jonathan Smallwood, Scott T. Grafton, and Jonathan W. Schooler. Regional White Matter
634 Variation Associated with Domain-specific Metacognitive Accuracy. *Journal of Cognitive Neuroscience*, 27(3):440–452,
635 March 2015.

636 44. Alan L. F. Lee, Eugene Ruby, Nathan Giles, and Hakwan Lau. Cross-Domain Association in Metacognitive Efficiency
637 Depends on First-Order Task Types. *Frontiers in Psychology*, 9, 2018.

638 45. Brian Maniscalco and Hakwan Lau. A signal detection theoretic approach for estimating metacognitive sensitivity from
639 confidence ratings. *Consciousness and Cognition*, 21(1):422–430, March 2012.

640 46. William Kruskal. Relative Importance by Averaging over Orderings. *The American Statistician*, 41(1):6–10, February 1987.

641 47. Ulrike Grömping. Estimators of Relative Importance in Linear Regression Based on Variance Decomposition. *The American
642 Statistician*, 61(2):139–147, May 2007.

643 48. Wendy E. Shields, J. David Smith, Katarina Guttmanova, and David A. Washburn. Confidence Judgments by Humans and
644 Rhesus Monkeys. *The Journal of general psychology*, 132(2):165–186, April 2005.

645 49. Shannon M. Locke, Michael S. Landy, and Pascal Mamassian. Suprathreshold perceptual decisions constrain models of
646 confidence. Technical report, PsyArXiv, December 2021. type: article.

647 50. Dobromir Rahnev, Tarryn Balsdon, Lucie Charles, Vincent de Gardelle, Rachel N. Denison, Kobe Desender, Nathan Faivre,
648 Elisa Filevich, Stephen Fleming, Janneke Jehee, Hakwan Lau, Alan L. F. Lee, Shannon M. Locke, Pascal Mamassian, Brian
649 Odegaard, Megan A. K. Peters, Gabriel Reyes, Marion Rouault, Jérôme Sackur, Jason Samaha, Claire Sergeant, Maxine
650 Sherman, Marta Siedlecka, David Soto, Alexandra Vlassova, and Ariel Zylberberg. Consensus goals for the field of visual
651 metacognition. Technical report, PsyArXiv, April 2021. type: article.

652 51. Yoshiaki Ko and Hakwan Lau. A detection theoretic explanation of blindsight suggests a link between conscious perception
653 and metacognition. *Philosophical Transactions of the Royal Society B: Biological Sciences*, 367(1594):1401–1411, May
654 2012.

655 52. Yutaka Komura, Akihiko Nikkuni, Noriko Hirashima, Teppei Uetake, and Aki Miyamoto. Responses of pulvinar neurons reflect
656 a subject's confidence in visual categorization. *Nature Neuroscience*, 16(6):749–755, June 2013.

657 53. Sébastien Massoni, Thibault Gajdos, and Jean-Christophe Vergnaud. Confidence measurement in the light of signal detec-
658 tion theory. *Frontiers in Psychology*, 5, 2014.

659 54. Ariel Zylberberg, Pablo Barttfeld, and Mariano Sigman. The construction of confidence in a perceptual decision. *Frontiers
660 in Integrative Neuroscience*, 6, 2012.

661 55. Brian Maniscalco, Megan A. K. Peters, and Hakwan Lau. Heuristic use of perceptual evidence leads to dissociation between
662 performance and metacognitive sensitivity. *Attention, Perception, & Psychophysics*, 78(3):923–937, April 2016.

663 56. Megan A. K. Peters, Thomas Thesen, Yoshiaki D. Ko, Brian Maniscalco, Chad Carlson, Matt Davidson, Werner Doyle, Ruben
664 Kuzniecky, Orrin Devinsky, Eric Halgren, and Hakwan Lau. Perceptual confidence neglects decision-incongruent evidence
665 in the brain. *Nature Human Behaviour*, 1(7):1–8, July 2017.

666 57. Stephen M. Fleming and Nathaniel D. Daw. Self-evaluation of decision-making: A general Bayesian framework for metacog-
667 nitive computation. *Psychological Review*, 124(1):91–114, 2017.

668 58. Christopher R. Fetsch, Roozbeh Kiani, and Michael N. Shadlen. Predicting the accuracy of a decision: a neural mechanism
669 of confidence. In *Cold Spring Harbor symposia on quantitative biology*, volume 79, pages 185–197. Cold Spring Harbor

670 Laboratory Press, 2014.

671 59. Peter R Murphy, Ian H Robertson, Siobhán Harty, and Redmond G O'Connell. Neural evidence accumulation persists after
672 choice to inform metacognitive judgments. *eLife*, 4:e11946, December 2015.

673 60. Koosha Khalvati, Roozbeh Kiani, and Rajesh P. N. Rao. Bayesian inference with incomplete knowledge explains perceptual
674 confidence and its deviations from accuracy. *Nature Communications*, 12(1):5704, September 2021.

675 61. Brian Maniscalco and Hakwan Lau. The signal processing architecture underlying subjective reports of sensory awareness.
676 *Neuroscience of Consciousness*, 2016(1), January 2016.

677 62. Armin Lak, Gil M. Costa, Erin Romberg, Alexei A. Koulakov, Zachary F. Mainen, and Adam Kepecs. Orbitofrontal Cortex Is
678 Required for Optimal Waiting Based on Decision Confidence. *Neuron*, 84(1):190–201, October 2014.

679 63. Roozbeh Kiani and Michael N. Shadlen. Representation of confidence associated with a decision by neurons in the parietal
680 cortex. *science*, 324(5928):759–764, 2009.

681 64. Joshua I. Sanders, Balázs Hangya, and Adam Kepecs. Signatures of a Statistical Computation in the Human Sense of
682 Confidence. *Neuron*, 90(3):499–506, May 2016.

683 65. Balázs Hangya, Joshua I. Sanders, and Adam Kepecs. A Mathematical Framework for Statistical Decision Confidence.
684 *Neural Computation*, 28(9):1840–1858, September 2016.

685 66. William T. Adler and Wei Ji Ma. Limitations of Proposed Signatures of Bayesian Confidence. *Neural Computation*,
686 30(12):3327–3354, December 2018.

687 67. Hsin-Hung Li and Wei Ji Ma. Confidence reports in decision-making with multiple alternatives violate the Bayesian confi-
688 dence hypothesis. *Nature Communications*, 11(1):2004, April 2020.

689 68. Laura S. Geurts, James R. H. Cooke, Ruben S. van Bergen, and Janneke F. M. Jehee. Subjective confidence reflects
690 representation of Bayesian probability in cortex. *Nature Human Behaviour*, pages 1–12, January 2022.

691 69. Benedetto De Martino, Stephen M. Fleming, Neil Garrett, and Raymond Dolan. Confidence in value-based choice. *Nature
692 neuroscience*, 16(1):105–110, January 2013.

693 70. Marc O. Ernst and Martin S. Banks. Humans integrate visual and haptic information in a statistically optimal fashion. *Nature*,
694 415(6870):429, 2002.

695 71. Christopher R. Fetsch, Alexandre Pouget, Gregory C. DeAngelis, and Dora E. Angelaki. Neural correlates of reliability-based
696 cue weighting during multisensory integration. *Nature neuroscience*, 15(1):146, 2012.

697 72. Ahmad T. Qamar, R. James Cotton, Ryan G. George, Jeffrey M. Beck, Eugenia Prezhdo, Allison Laudano, Andreas S. Tolias,
698 and Wei Ji Ma. Trial-to-trial, uncertainty-based adjustment of decision boundaries in visual categorization. *Proceedings of
699 the National Academy of Sciences*, 110(50):20332–20337, December 2013.

700 73. Wei Ji Ma, Jeffrey M. Beck, Peter E. Latham, and Alexandre Pouget. Bayesian inference with probabilistic population codes.
701 *Nature neuroscience*, 9(11):1432, 2006.

702 74. Gergő Orbán, Pietro Berkes, József Fiser, and Máté Lengyel. Neural variability and sampling-based probabilistic represen-
703 tations in the visual cortex. *Neuron*, 92(2):530–543, 2016.

704 75. Ruben S. van Bergen, Wei Ji Ma, Michael S. Pratte, and Janneke F. M. Jehee. Sensory uncertainty decoded from visual
705 cortex predicts behavior. *Nature Neuroscience*, 18(12):1728–1730, December 2015.

706 76. Olivier J. Hénaff, Zoe M. Boundy-Singer, Kristof Meding, Corey M. Ziemba, and Robbe L. T. Goris. Representation of visual
707 uncertainty through neural gain variability. *Nature Communications*, 11(1):2513, May 2020.

708 77. Edgar Y. Walker, R. James Cotton, Wei Ji Ma, and Andreas S. Tolias. A neural basis of probabilistic computation in visual
709 cortex. *Nature Neuroscience*, 23(1):122–129, January 2020.

710 78. Dylan Festa, Amir Aschner, Aida Davila, Adam Kohn, and Ruben Coen-Cagli. Neuronal variability reflects probabilistic
711 inference tuned to natural image statistics. *Nature Communications*, 12(1):3635, June 2021.

712 79. Ariel Zylberberg, Pieter R. Roelfsema, and Mariano Sigman. Variance misperception explains illusions of confidence in
713 simple perceptual decisions. *Consciousness and Cognition*, 27:246–253, July 2014.

714 80. Ariel Zylberberg, Christopher R Fetsch, and Michael N Shadlen. The influence of evidence volatility on choice, reaction time
715 and confidence in a perceptual decision. *eLife*, 5:e17688, October 2016.

716 81. Santiago Herce Castañón, Rani Moran, Jacqueline Ding, Tobias Egner, Dan Bang, and Christopher Summerfield. Human
717 noise blindness drives suboptimal cognitive inference. *Nature Communications*, 10(1):1719, April 2019.

718 82. John Palmer, Alexander C. Huk, and Michael N. Shadlen. The effect of stimulus strength on the speed and accuracy of a
719 perceptual decision. *Journal of Vision*, 5(5):1, May 2005.

720 83. Timothy D. Hanks, Mark E. Mazurek, Roozbeh Kiani, Elisabeth Hopp, and Michael N. Shadlen. Elapsed Decision Time
721 Affects the Weighting of Prior Probability in a Perceptual Decision Task. *Journal of Neuroscience*, 31(17):6339–6352, April
722 2011.

723 84. Roozbeh Kiani, Leah Cortell, and Michael N. Shadlen. Choice Certainty Is Informed by Both Evidence and Decision Time.
724 *Neuron*, 84(6):1329–1342, December 2014.

725 85. John Gibbon. Scalar expectancy theory and Weber's law in animal timing. *Psychological Review*, 84(3):279–325, 1977.

726 86. Mehrdad Jazayeri and Michael N. Shadlen. Temporal context calibrates interval timing. *Nature Neuroscience*, 13(8):1020–
727 1026, August 2010.

728 87. Mehrdad Jazayeri and Michael N. Shadlen. A Neural Mechanism for Sensing and Reproducing a Time Interval. *Current
729 Biology*, 25(20):2599–2609, October 2015.

730 88. Wilson S. Geisler. Ideal observer analysis. In *The Visual Neurosciences*, volume 10, pages 825–837. MIT Press, Boston,
731 2003.

732 89. Yair Weiss, Eero P. Simoncelli, and Edward H. Adelson. Motion illusions as optimal percepts. *Nature neuroscience*, 5(6):598,
733 2002.

734 90. Navindra Persaud, Peter McLeod, and Alan Cowey. Post-decision wagering objectively measures awareness. *Nature
735 Neuroscience*, 10(2):257–261, February 2007.

736 91. Zoltán Dienes and Anil Seth. Gambling on the unconscious: A comparison of wagering and confidence ratings as measures
737 of awareness in an artificial grammar task. *Consciousness and Cognition*, 19(2):674–681, June 2010.

738 92. Zahra Murad, Martin Sefton, and Chris Starmer. How do risk attitudes affect measured confidence? *Journal of Risk and
739 Uncertainty*, 52(1):21–46, February 2016.

740 93. F. A. Wichmann and N. J. Hill. The psychometric function: I. Fitting, sampling, and goodness of fit. *Perception & Psy-
741 chophysics*, 63(8):1293–1313, November 2001.

742 Acknowledgements

743 We thank the creators and contributors to the Confidence Database and Joaquin Navajas for making their data available. This
744 work was supported by a U.S. National Science Foundation Graduate Research Fellowship (to ZMB-S), U.S. National Institutes
745 of Health grants T32 EY021462 (supporting CMZ), K99 EY032102 (to CMZ), and EY032999 (to RLTG), and a Whitehall
746 Foundation grant (to RLTG).

747 Author contributions

748 ZMB-S, CMZ, and RLTG conceived the study, developed the theory, performed the simulations, analyzed the data, and wrote
749 the paper.

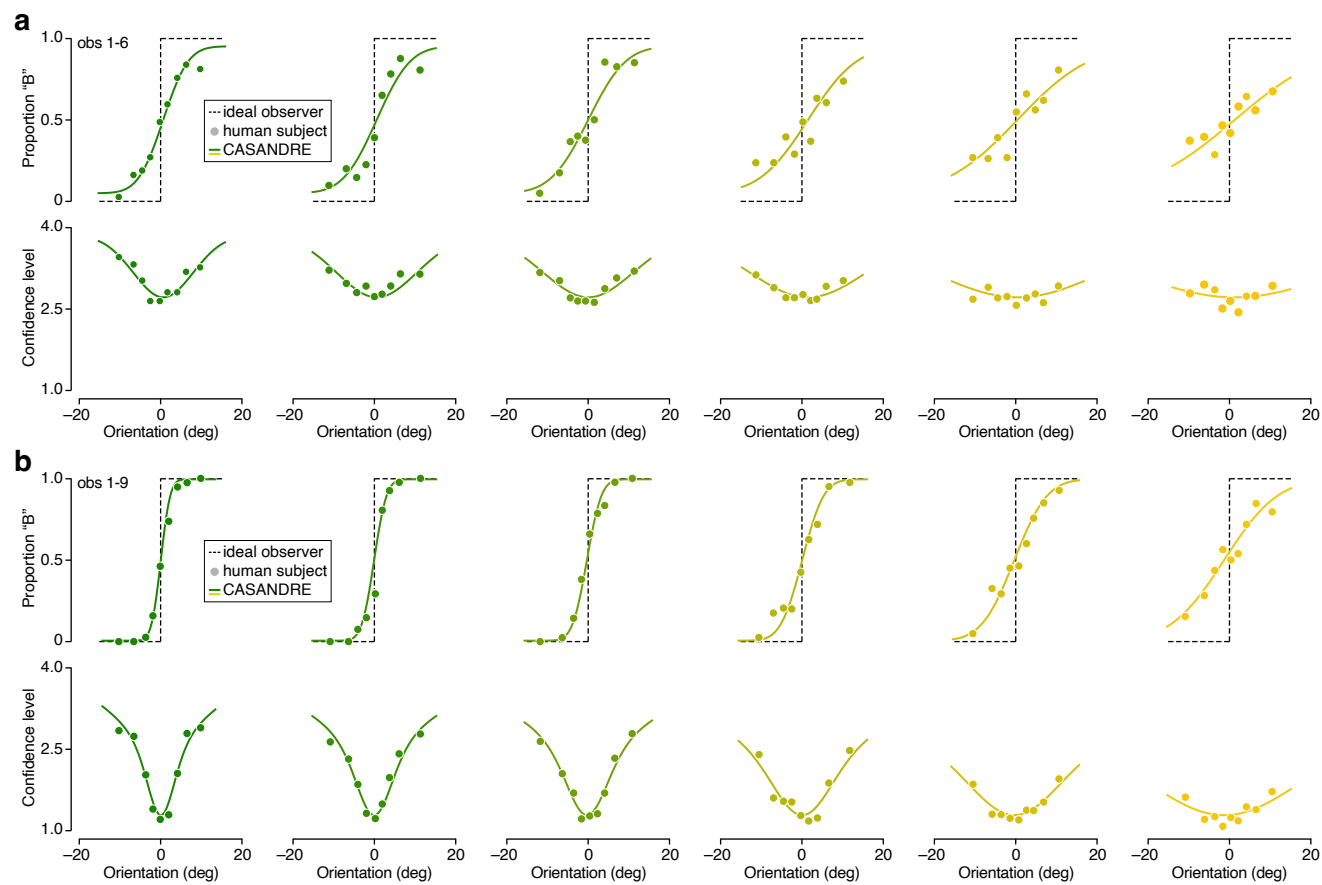
750 Competing interests

751 The authors declare no competing interests.

752 Supplementary information

753 Adler and Ma (2018), task 1

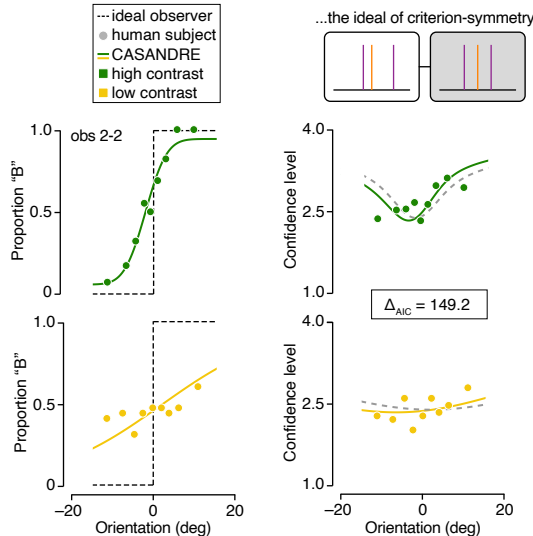
754 Figure 1b,c shows data from two subjects who performed a perceptual 2-AFC categorization task and additionally reported
 755 their confidence using a four-point rating scale. Data were collected by Adler and Ma (2018). Supplementary Figure 1a,b
 756 illustrates model fits by plotting the psychometric function (top row) and accompanying confidence function (bottom row) for
 757 each stimulus contrast (columns). Subjects completed 2,160 trials each. To model these data, we used one lapse rate parameter
 758 (obs 1-6: 5%; obs 1-9: 0.5%), one contrast-specific sensitivity parameter (obs 1-6: 0.21, 0.15, 0.14, 0.11, 0.07, and 0.06; obs
 759 1-9: 0.55, 0.42, 0.36, 0.24, 0.16, and 0.10), one contrast-specific decision criterion parameter (obs 1-6: 0.62, 0.55, 0.00, 1.49,
 760 0.45, and 1.28 degrees; obs 1-9: 0.03, -0.08, -0.32, 0.05, -0.35, and -1.33 degrees), one meta-uncertainty parameter (obs 1-6:
 761 0.21; obs 1-9: 0.51), and three confidence criterion parameters (obs 1-6: 0.02, 0.40, and 1.92; obs 1-9: 1.42, 3.30, and 10.99).
 762 The log-probability of the data under the model was -3,462.1 for obs 1-6, and -2,654.0 for obs 1-9.



Supplementary Figure 1 Model fits for two example subjects from Adler and Ma (2018). Both subjects judged whether a stimulus belonged to category A or B. Category A stimuli typically had an orientation smaller than zero, while category B stimuli typically had an orientation larger than zero. Stimuli varied in orientation and contrast. **(a)** Top: Proportion of "Category B" choices is plotted against stimulus orientation, split out by stimulus contrast (columns, contrast decreases from left to right), for one example subject (observer 6 in experiment 1 from ref. ²⁵). Bottom: Same for mean confidence level. Symbols summarize observed choice behavior, the dotted line illustrates the theoretical optimum, and the full lines show the fit of a two-stage process model of decision-making. Symbol size is proportional to the number of trials. **(b)** Same for a different example subject (observer 9 in experiment 1 from ref. ²⁵).

763 **Evaluating the ideal of criterion-symmetry**

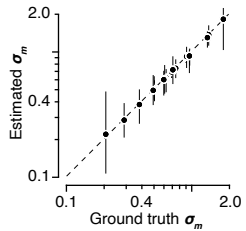
764 Figure 3a,b shows data for one example subject (2-7) from Adler and Ma (2018) fit with different model variants. This
765 example subject's data were marginally better fit with a model with asymmetrical rather than symmetric confidence criteria
766 (AIC difference = 10.9). Supplementary Figure 2 illustrates data from another example subject (2-2) for whom the difference
767 in model performance is more substantial (AIC difference = 149.2).



Supplementary Figure 2 Following the same conventions as Figure 3. Left: proportion of "Category B" choices is plotted against stimulus orientation for high contrast (top, green) and low contrast (bottom, yellow) for example subject (observer 2 in experiment 2 from ref. ²⁵). Right: Mean confidence level is plotted as a function of stimulus orientation for the same example observer. Symbols indicate data; lines indicate model fits. Solid lines indicate CASANDRE model fit with asymmetric confidence criteria. Dashed lines indicate CASANDRE model fit with symmetric confidence criteria.

768 **Meta-uncertainty recovery, Adler and Ma (2018) task 1**

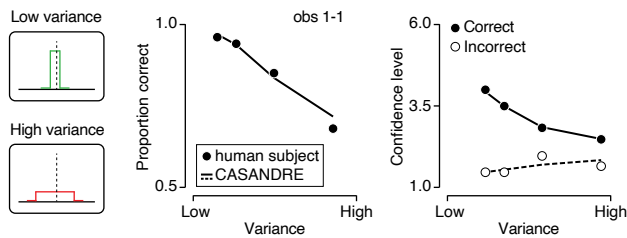
769 We verified that meta-uncertainty can be reliably recovered for the datasets used to evaluate the model's architecture. These
770 datasets came from the 19 subjects who participated in ref. 25's experiment 1 and 2. For each subject, we simulated 100 choice-
771 confidence datasets using the CASANDRE model and the best-fitting parameter values. Each simulated experiment exactly
772 matched the set of trials completed by the subject. We then analyzed the synthetic data in the same manner as the real data. As
773 can be seen in Supplementary Figure 3, under this experimental design, meta-uncertainty is recoverable.



Supplementary Figure 3 Model recovery analysis for Adler and Ma (2018) task 1 data. The median estimate of meta-uncertainty is plotted against the ground truth value for each subject. Error bars illustrate the interquartile range (IQR) computed from 100 simulated data sets.

774 **Navajas et al. (2017), experiment 1**

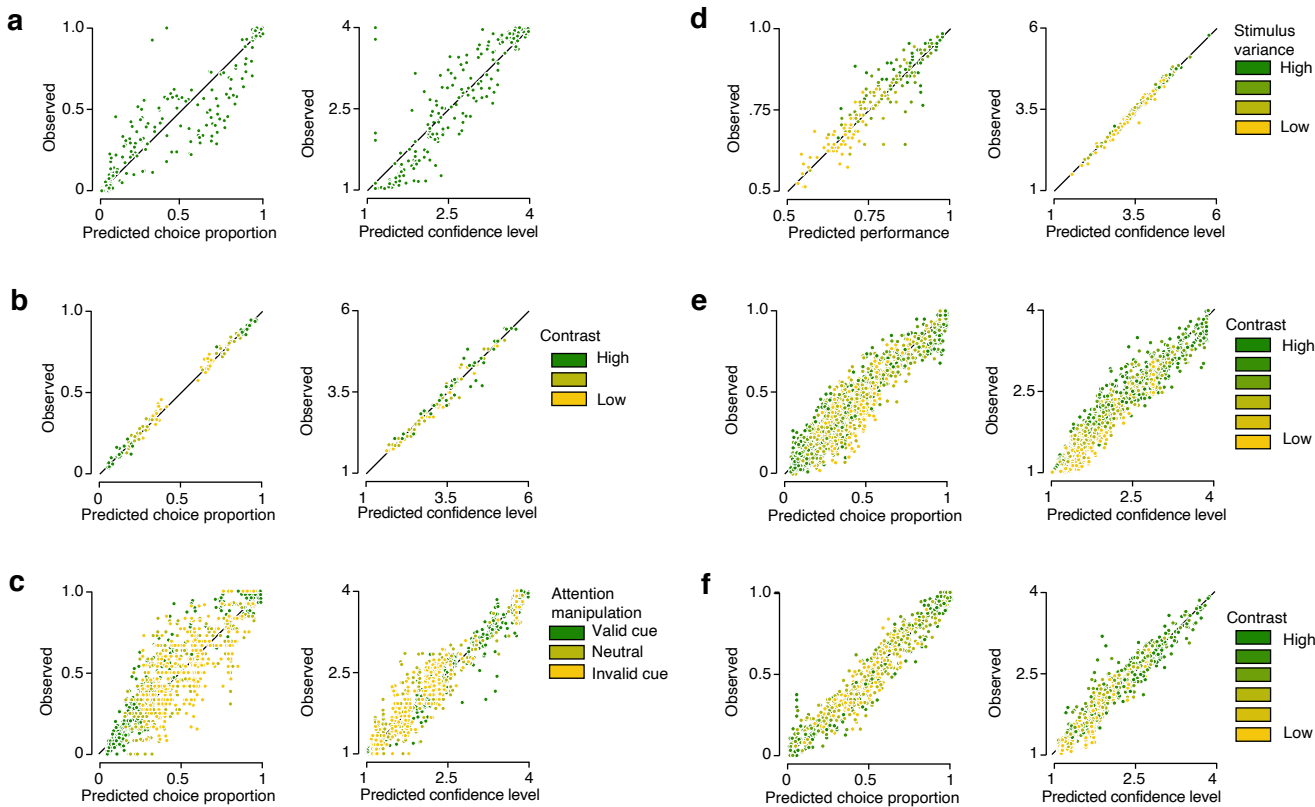
775 Figure 5a-d shows an analysis of data from subjects who performed either a perceptual or cognitive 2-AFC categorization
776 task and additionally reported their confidence using a six-point rating scale. Data were collected by Navajas et al. (2017).
777 Supplementary Figure 4 illustrates the model fit for an example subject by plotting the data in the format used in the original
778 publication²⁴. Proportion correct and confidence level are plotted against stimulus variance. The confidence reports are split
779 out by decision accuracy. The experiment consisted of 400 trials. To model these data, we used one lapse rate parameter
780 (0%), one stimulus variance-specific sensitivity parameter (0.67, 0.53, 0.33, and 0.19), one decision criterion parameter (-0.59
781 degrees), one meta-uncertainty parameter (0.10), and five confidence criterion parameters (0.35, 1.19, 1.64, 2.29, and 3.36).
782 The log-probability of the data under the model was -733.50.



Supplementary Figure 4 Model fit for an example subject from Navajas et al. (2017) (observer 1 in experiment 1). The subject judged whether the mean orientation of a sequence of 30 rapidly presented Gabor stimuli was tilted right or left. Left: Stimulus sequences were sampled from distributions with different orientation variance. Middle: Proportion correct choices is plotted against stimulus variance for an example subject. Right: Mean confidence level is plotted against stimulus variance, split out by decision accuracy. Symbols summarize observed choice behavior, the full line shows the fit of a two-stage process model of decision-making.

783 **Goodness-of-fit across datasets**

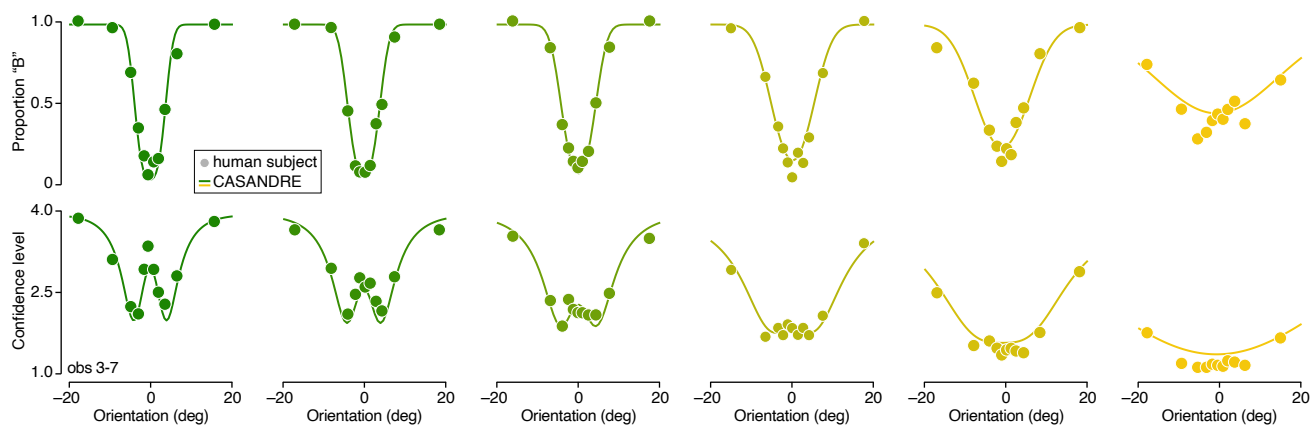
784 Supplementary Figure 5 shows a comparison of the model predicted and observed choice behavior and confidence reports for
 785 the six tasks included in figure 7c.



Supplementary Figure 5 Each symbol summarizes a single stimulus condition for a single subject. Color indicates stimulus reliability. Left: Observed versus predicted choice behavior. Right: Observed versus predicted confidence level. **(a)** Data from Rausch et al. (2020): 25 subjects. **(b)** Shekhar and Rahnev (2021): 20 subjects. **(c)** Denison et al. (2018): 12 subjects. **(d)** Navajas et al. (2017): 50 subjects; **e** Adler and Ma (2018) task 2: 34 subjects; **f** Adler and Ma (2018) task 1: 19 subjects;

786 **Adler and Ma (2018), task 2**

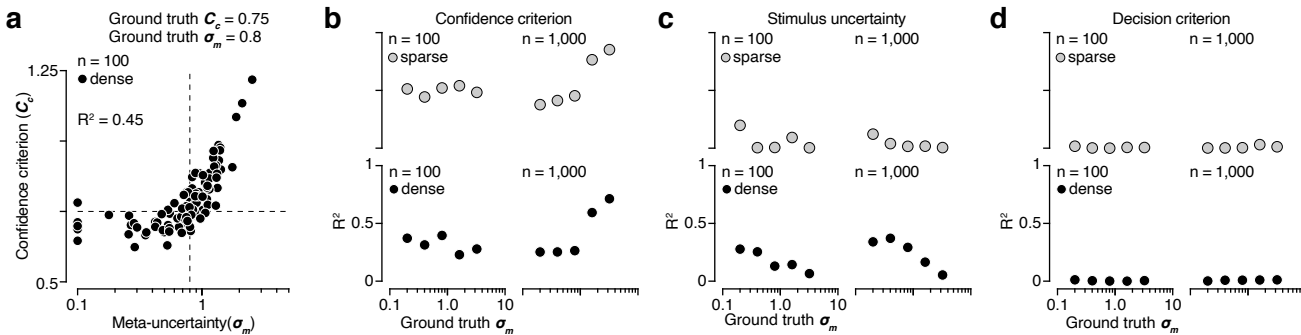
787 Figure 7c includes a data-point for task 2 from Adler and Ma (2018) and one for Denison et al. (2018). Both studies employed
788 a task design in which subjects discriminated two categories of orientation distributions with the same mean but different
789 standard deviations. Supplementary Figure 6 illustrates an example model fit for this task by plotting the psychometric function
790 (top row) and accompanying confidence function (bottom row) for each stimulus contrast (columns). The subject completed
791 3,240 trials. To model these data, we used one lapse rate parameter (2.17%), one contrast-specific sensitivity parameter (0.68,
792 0.55, 0.46, 0.28, 0.20, and 0.07), one contrast-specific low decision criterion parameter (-4.05, -4.27, -4.35, -5.21, -7.30, and
793 -11.34 degrees), one contrast-specific high decision criterion parameter (3.62, 3.76, 4.26, 5.36, 5.38, and 9.66 degrees), one
794 meta-uncertainty parameter (0.69), three confidence criterion parameters for “Category A” choices (0.69, 1.15, and 1.89), and
795 three confidence criterion parameters for “Category B” choices (0.65, 1.78, and 4.53). The log-probability of the data under the
796 model was -4,842.5. (Note: while the model fit illustrated here employs asymmetric confidence criteria, all fits in Figure 7c
797 were with symmetric confidence criteria for consistency.)



Supplementary Figure 6 Model fits for an example subject from Adler and Ma (2018) (observer 7 in experiment 3). The subject judged whether a stimulus belonged to category A or B. Category A stimuli were drawn from a distribution with small orientation spread, category B stimuli were drawn from a distribution with large orientation spread. Stimuli varied in orientation and contrast. Top: Proportion of “Category B” choices is plotted against stimulus orientation, split out by stimulus contrast (columns, contrast decreases from left to right), for one example subject. Bottom: Same for mean confidence level. Symbols summarize observed choice behavior, the full lines show the fit of the CASANDRE model.

798 Parameter trade-offs

799 Figure 4 illustrates a recovery analysis for the meta-uncertainty parameter of the CASANDRE model. Supplementary Figure 7
 800 illustrates an additional analysis of the trade-off between meta-uncertainty and the other parameters of the CASANDRE model
 801 using the same generated data and model fits as in Figure 4c. Although the variance in meta-uncertainty explained by trade-
 802 offs with confidence criterion can reach high levels, this is somewhat mitigated by denser stimulus sampling (Supplementary
 803 Fig. 7b, bottom) and is reasonable for datasets with a larger number of trials (Supplementary Fig. 7b, right) and for values of
 804 meta-uncertainty that are empirically observed more often (less than 1).



Supplementary Figure 7 Trade-off between meta-uncertainty and other CASANDRE model parameters. **(a)** Parameter correlation for an example condition. Recovered meta-uncertainty and confidence criterion are plotted against each other for 100 model-generated datasets. The dashed lines represent the ground truth values for confidence criterion ($C_c = 0.75$) and meta-uncertainty ($\sigma_m = 0.8$). Each symbol represents one dataset generated with 100 trials and a dense stimulus sampling regime. **(b)** Trade-off between meta-uncertainty and confidence criterion. **(c)** Trade-off between meta-uncertainty and stimulus uncertainty. **(d)** Trade-off between meta-uncertainty and decision criterion.)

805 Comparison with a criteria-noise model

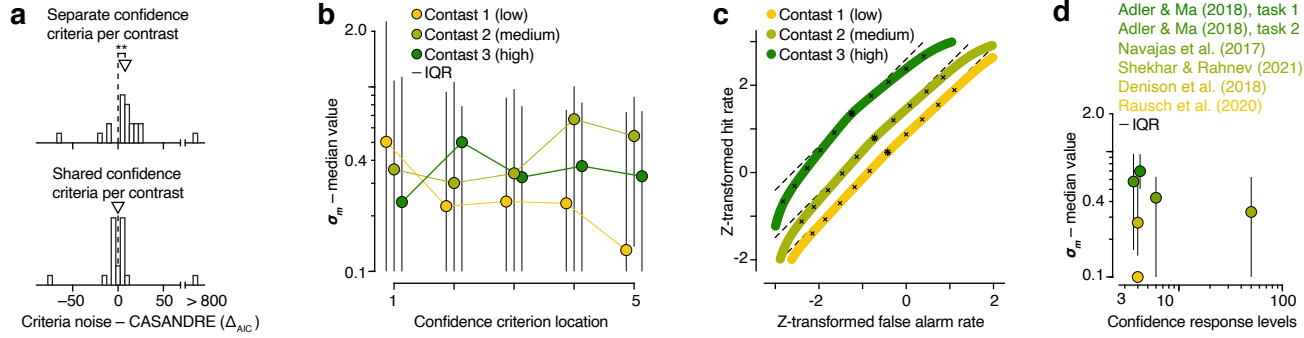
806 Shekhar and Rahnev recently described a hierarchical process model of confidence with desirable properties that dissociate
807 a parameter capturing metacognitive ability from stimulus sensitivity and confidence reporting strategy²⁸. They refer to the
808 parameter capturing metacognitive ability as “meta-noise” and find that log-normally distributed meta-noise provides a better
809 quantitative and qualitative match to empirical data than normally distributed noise. In the CASANDRE model, the standard
810 deviation of a log-normal distribution also serves as a metric for the metacognitive ability of an observer, however these two
811 uses of log-normal noise, like the models themselves, are not equivalent. In the CASANDRE model, the confidence variable
812 is distributed according to the ratio of a normally and log-normally distributed variable, whereas in the model of Shekhar and
813 Rahnev the confidence variable has a normal distribution identical to the decision variable but the positions of the confidence
814 criteria are subject to log-normally distributed noise. We thus refer to the model of Shekhar and Rahnev as the “criteria-noise”
815 model.

816 We quantitatively compared the criteria-noise model with the CASANDRE model. Because the criteria-noise model is currently
817 limited to experiments with two stimulus strengths, we did not apply it to data from ref. ²⁵ (as we did for comparing other
818 model variants in Fig. 3), but instead fit the CASANDRE model to the data reported in their original paper²⁸. For purposes of
819 quantitative comparison to the criteria-noise model, we fit the CASANDRE model with asymmetric confidence criteria (yielding
820 15 total parameters, see Methods). First, we compared the CASANDRE model to the criteria-noise model as described by
821 Shekhar and Rhanev, with a different set of confidence criteria for each of three contrast values (yielding 35 total parameters).
822 The CASANDRE model significantly outperformed the criteria-noise model (median difference in AIC = 7.8; $P = 0.002$,
823 Wilcoxon signed-rank test; Supplementary Fig. 8a, top). Second, we compared the CASANDRE model to a simpler version
824 of the criteria-noise model with only one set of confidence critiera (yielding 15 total parameters). There was no difference in
825 performance between the CASANDRE model and this variant of the criteria-noise model (median difference in AIC = -0.1; P
826 = 1, Wilcoxon signed-rank test; Supplementary Fig. 8a, bottom). Note: we discovered an incorrect scaling of likelihood values
827 in the original code accompanying ref. ²⁸. We fixed this scaling and thus the AIC values used in this model comparison for the
828 criteria-noise model differ from those reported in ref. ²⁸.

829 Shekhar and Rahnev demonstrated that the level of confidence criteria noise can serve as a measure of metacognitive ability
830 uncontaminated by stimulus sensitivity or confidence reporting strategy²⁸. For comparison, we performed the same analysis
831 using the CASANDRE model. Following their procedure, we mapped each subject’s continuous confidence reports into five
832 different binary confidence rating scales, biasing confident reports to be more liberal or conservative. For each subject, we fit
833 the CASANDRE model independently to each of these five remapped datasets across the three contrast levels. We removed one
834 subject that in some conditions did not generate a single response to one of the four possible response options. Meta-uncertainty
835 was largely insensitive to both confidence reporting strategy and stimulus sensitivity (Supplementary Fig. 8b; compare to Fig.
836 11a in Shekhar and Rahnev²⁸). A two-way ANOVA revealed no main effect of confidence criterion ($F(4, 18) = 1.97, P = 0.11$)
837 or stimulus contrast ($F(2, 18) = 0.04, P = 0.96$) on meta-uncertainty. Further, the interaction between confidence reporting
838 strategy and stimulus sensitivity was not significant ($F(2, 4) = 1.57, P = 0.14$). These results along with the model comparison
839 (Supplementary Fig. 8a) demonstrate that the CASANDRE model performs quantitatively at least as well as the criteria-noise
840 model in explaining the data reported in ref. ²⁸.

841 We now turn to several more qualitative considerations that favor the CASANDRE model compared with the criteria-noise
842 model. First, Shekhar and Rahnev show that empirical, averaged zROC functions have significant curvature compared with the
843 straight zROC functions predicted by signal detection theory (their Fig. 4 and 5b). The criteria-noise model shows curved zROC
844 functions but, as the authors note, they resemble piecewise linear functions rather than the smoothly curving zROC functions
845 of the empirical data (see their Fig. 11, bottom left). The CASANDRE model generates smoothly curving averaged zROC
846 functions that more closely resemble the empirically estimated zROC curves (Supplementary Fig. 8c; compare with Fig. 4 and
847 5b in ref. ²⁸). Second, the CASANDRE model is easier to fit to data given that its parameters can be optimized using standard
848 maximum likelihood estimation procedures, rather than the purpose-built, two-stage parameter search algorithm developed by
849 Shekhar and Rahnev. Third, the CASANDRE model is more general and can be applied to experiments that vary stimulus
850 strength in addition to stimulus uncertainty (such as ref. ²⁵), whereas the criteria-noise model is limited to experiments with two
851 stimulus strengths. This is because the criteria-noise model makes the assumption that confidence is measured in units of d' , but
852 does not specify the computation that transforms units of stimulus to units of d' . Fourth, the CASANDRE model specifies this
853 confidence computation and posits that it is exactly noise in this transformation that can lead to limited metacognitive ability.
854 Analogous to stimulus discrimination ability being limited by variation in the estimation of the stimulus, the CASANDRE
855 model posits that metacognition is limited by variation in the estimation of the uncertainty required to compute confidence.
856 In contrast, the criteria-noise model posits that lower metacognitive ability arises from the inability of subjects to maintain
857 constant confidence criteria. Stochastic confidence criteria cause problems for model tractability, allowing for them to cross
858 both the decision criterion and each other. By casting criteria-noise as log-normally distributed, Shekhar and Rahnev avoid the

problem of crossovers with the decision criterion, but to solve the problem of crossovers between confidence criteria they make the questionable assumption that noise is perfectly correlated across criteria. The CASANDRE model naturally avoids both of these issues. Fifth, the process captured by the CASANDRE model leads to new predictions about how metacognitive ability can be experimentally manipulated. Figure 7 illustrates how increasing the number of uncertainty levels in a task increases meta-uncertainty. If an inability to maintain stable criteria were a source of lower metacognitive ability instead, increasing the number of confidence response levels on the rating scale used by subjects should lower metacognitive ability (and increase meta-uncertainty estimated from the CASANDRE model). We see no evidence for this prediction when rearranging the estimated meta-uncertainty across tasks according to the number confidence response levels (Supplementary Fig. 8d).



Supplementary Figure 8 Comparison with Shekhar and Rahnev (2021). **(a)** Distribution of the difference in AIC value across 20 subjects for the CASANDRE model compared with the criteria-noise model with a different set of confidence criteria for each of three contrast levels (top) or with one shared set of confidence criteria across all three contrasts (bottom). Positive values indicate evidence favoring the CASANDRE model. Arrows indicate the median of the distribution. ** $P < 0.01$, Wilcoxon signed-rank test. **(b)** Median meta-uncertainty across 20 subjects estimated independently for each contrast and confidence criterion location. Error bars illustrate the interquartile range (IQR) across subjects. Compare to Fig. 11a in ref. ²⁸. **(c)** Averaged zROC functions across 20 subjects generated from fits of the CASANDRE model. The location of the decision criterion is indicated by an asterisk, and the location of each confidence criterion is indicated by an x. The dashed lines illustrate the linear zROC functions predicted from signal detection theory. Compare to Fig. 4, 5b, and 10 in ref. ²⁸. **(d)** Median level of meta-uncertainty plotted against number of confidence response levels for six confidence experiments. Error bars illustrate the interquartile range (IQR) across subjects. Note the symbol representing ref. ²⁸ is plotted at 50 although subjects rated their confidence on a continuous scale ranging from 50-100.